

ECONOMIC GEOLOGY

AND THE

BULLETIN OF THE SOCIETY OF ECONOMIC GEOLOGISTS

VOL. 92

May, 1997

No. 3

An Amagmatic Origin of Carlin-Type Gold Deposits

ROBERT P. ILCHIK* AND MARK D. BARTON

Center for Mineral Resources, Department of Geosciences, University of Arizona, Tucson, Arizona 85721

Abstract

Carlin-type deposits are major sources of gold, yet their origins are enigmatic. Suggested genetic models make connections to magmatism, regional metamorphism, or regional extension. Depositional mechanisms are uncertain as well. We propose on the basis of geologic, physical, and chemical reasoning, a genetic model in which meteoric fluids were circulated by heat released during crustal extension. These fluids interacted at depth with the sedimentary rock pile and scavenged gold. Upon upwelling, these fluids interacted with various lithologies and/or other fluids and produced the characteristic alteration and metal suites of these deposits. To test the viability of this amagmatic model, we have investigated certain physical and chemical constraints implicit to the model.

Heat balance calculations indicate that ample surface waters could be heated to appropriate temperatures and circulated during rapid crustal extension. Mass balance calculations indicate that solution transport efficiencies of <10 percent can account for several times the amount of known alteration and mineralization. In contrast, magma-driven or metamorphic fluids appear to be less adequate sources.

A two-step, source to deposit approach was used to simulate fluid-rock interaction and mass transport implied in the amagmatic model. Fluids with a fixed ΣCl were first equilibrated with various potential source rocks (arkose, graywacke, and pelite, each with various f_{O_2} and f_{S_2} buffer assemblages) at 300°C and 1 kbar to simulate reaction at depth, perhaps near the brittle-ductile transition. These fluids were then reequilibrated under conditions indicated for deposit formation (225°–150°C, 0.5 kbars) to investigate processes including cooling, wall-rock reaction, and mixing which could be important to ore deposition. Gold transport was favored for low-chlorinity, intermediate oxidation state (below pyrrhotite-pyrite-magnetite), slightly acid fluids from sulfide-bearing sources (i.e., equilibration with arkosic rocks). These conditions are not conducive to base metal transport and explain the rarity of base metals in Carlin-type systems. When reacted under deposit level conditions, these calculated ore fluids leach carbonate and deposit quartz. The volume ratio of carbonate dissolved to quartz precipitated is ~0.2 to 2.5, and increases when mixing with a second fluid is considered. Arkose-equilibrated source fluids can precipitate gold by combinations of wall-rock reaction with a decarbonated host, mixing with various sulfide-poor fluids, and reaction with iron-rich host rocks. Cooling alone is ineffective over this temperature interval. Although most deposits are hosted by decarbonated marls, geochemical calculations suggest that other depositional environments are feasible, consistent with observation. Although here applied to the amagmatic hypothesis, these chemical calculations are not mechanism specific and might also be appropriate to metamorphic or magma-driven hydrothermal systems.

These results demonstrate that Carlin-type deposits can result from the coincidence of an effective driving force (rapid, major crustal extension), a source of dilute fluids, and chemically appropriate sets of both source and host rocks. The aqueous chemistry involved is unexceptional and shares many features with other types of moderate- to low-temperature gold-bearing hydrothermal systems—it is the geologic setting, and perhaps the fluid driving force, that is unusual. An amagmatic model is consistent with both deposit-scale and regional-scale observations; it rationalizes Carlin-type systems in the framework of southwestern North American metallogeny and it implies multiple possible mechanisms for gold mineralization. Detachment-type gold systems may be the high-oxidation state, high-salinity analogues of Carlin-type systems, formed by major extension, but from contrasting lithologic and fluid sources.

Introduction

CARLIN-TYPE gold deposits are widespread throughout much of the north-central and northeastern Basin and Range province of western North America (Fig. 1). They have been a major source of Nevada gold production for much of this century, and currently rank as the foremost gold producers

in the United States. Descriptions of a number of deposits establish many of their general characteristics reasonably well (see reviews by and references in Bagby and Berger, 1985; Tooker, 1985; Ilchik and Barton, 1996). Despite their economic importance and rather lengthy history of development, a consensus on the genesis of these deposits has not been achieved.

Three contrasting genetic models draw parallels with better understood magmatic hydrothermal or metamorphic gold-

* Current address: Either Ore, 1631 Foster Drive, Reno, NV 89509.

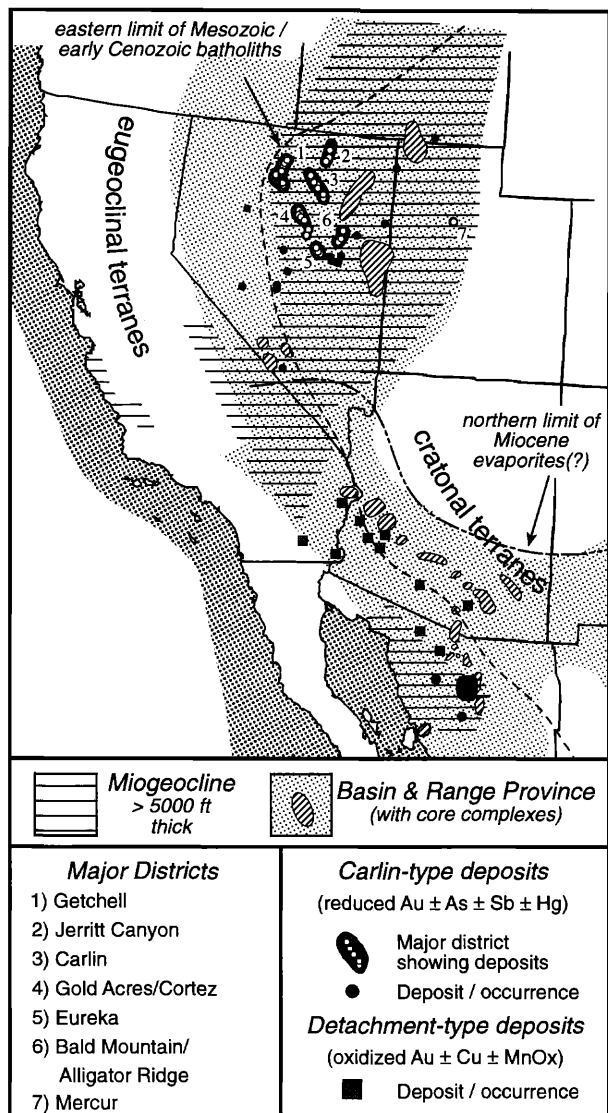


FIG. 1. Location map for Carlin-type and detachment-type gold deposits in western North America shown in relation to Cenozoic features of the Basin and Range and nearby geologic provinces. Deposit locations are from Percival et al. (1988), Barton et al. (1988), Raines et al. (1991), and Staudé (1995).

bearing systems (Seedorff, 1991), or invoke alternative mechanisms to drive hydrothermal circulation (Ilchik, 1990b). The first hypothesis suggests that Carlin-type deposits are distal portions of magmatic hydrothermal systems and proposes that magmas drive hydrothermal circulation and are the source for some fluid components and metals (Radtke et al., 1980; Alvarez and Noble, 1988; Sillitoe and Bonham, 1990; Arehart et al., 1993a). A second model draws parallels with many models for mesothermal gold deposits and suggests that major fluid components and metals were derived during regional metamorphism of supercrustal rocks (Seedorff, 1991; Phillips and Powell, 1993).

A third hypothesis, the focus of this paper, is that Carlin-type deposits develop in (meta)sedimentary rock-dominated terranes as a consequence of regional fluid circulation due to

crustal extension. No link to magmatism or other heating events is necessary. The amagmatic hypothesis derives from the lack of strong association with igneous activity and from the apparent temporal, chemical, and physical connection with crustal extension and (meta)sedimentary sources. Circulation of meteoric water is a response to extension-caused elevation of the geotherm and increases in permeability. Metals, sulfur, and silica are scavenged from sedimentary rocks at depth and are deposited in chemically favorable environments as the fluids ascend. Crustal extension is a net cooling process because no heat is added to the crust, nevertheless crustal thinning raises the geothermal gradient as burial depths diminish (cf. Dokka and Baski, 1988). Other heat sources (i.e., magmatism) would enhance the overall process, but they are not required.

In this paper, we briefly compare an amagmatic model, along with magmatic and metamorphic models, to the regional framework of the Great Basin and deposit-scale geology of Carlin-type deposits. We then focus on the physical and chemical consequences of the amagmatic model. Regional characteristics are used to assess the ability of mid-Tertiary extension to drive hydrothermal circulation. The geochemical consequences of amagmatic hydrothermal circulation are assessed using numerical simulations of hydrothermal scavenging, transport, and deposition of gold and other constituents within a low-metamorphic-grade sedimentary succession. We conclude with an examination of some of the metallogenic implications for the Great Basin and surrounding areas.

Regional Framework

Three features of the Great Basin are central to the various models for the development of Carlin-type deposits: first, the Cordilleran miogeocline which represents the host and possible source rocks for mineralization; second, widespread late Mesozoic and mid-Tertiary magmatism, which has various relationships with multiple types of hydrothermal systems; and third, pronounced mid-Tertiary extension which, with or without accompanying magmatism, promoted hydrothermal circulation.

The first component, the Cordilleran miogeocline, accumulated following Late Proterozoic rifting on the western margin of North America (Fig. 1; Stewart, 1980). The base of the miogeocline consists of 5 to 8 km of syn- to poststratifying, commonly reduced (carbonaceous, sulfide-bearing) clastic metasedimentary rocks, primarily metapelites and quartzites. Overlying the clastic section, limestones and dolostones dominate the Cambrian through Upper Devonian sections of the continental shelf, whereas mixed carbonate and siliciclastic rocks formed to the west on the slope. Passive margin sedimentation was interrupted by the Late Devonian Antler orogeny and was terminated by the Late Permian to Early Triassic Sonoma orogeny (Miller et al., 1992). Mesozoic tectonism was both compressional and extensional, with neutral to extensional regimes in the early Mesozoic giving way to compressional regimes of the Sevier orogeny in the late Mesozoic (Saleeby and Busby-Spera, 1992). This tectonism was accompanied by sporadic plutonism in the central Great Basin which lay in the hinterland of the Mesozoic arcs (Barton et al., 1988). Associated with these intrusions are various styles of porphyry, skarn, and replacement mineralization, some of

which are gold rich (Smith et al., 1988; Barton, 1990; Barton et al., 1993). It is these intrusions which have been related to Carlin-type mineralization in some studies (e.g., Arehart et al., 1993a).

Following magmatic and tectonic quiescence during much of the Laramide orogeny (~80–40 Ma), major mid-Tertiary extension was accompanied by voluminous calc-alkaline magmatism (Gans et al., 1989). Extension, locally up to 400 percent but averaging 50 to 100 percent, was marked by the development of ductile shear in the middle crust and normal faulting in the upper crust and was most extreme around metamorphic core complexes (e.g., Gans and Miller, 1983; Dickinson, 1991). Extension in the Great Basin began in the northeast at ~42 Ma, migrated to the south and west through the Oligocene and early Miocene, and is unevenly developed across the region (Seedorff, 1991). In the northern Great Basin, volcanic rocks and subjacent stocks constitute ~20 percent and ~1 percent of exposed bedrock, respectively (Stewart and Carlson, 1978). This magmatism most likely aided the extensional processes by heating the middle crust and, to the extent that juvenile magmatic material was added, would have partially compensated for the crustal attenuation due to extension (e.g., Gans et al., 1989).

Both magmatism and extension elevated thermal gradients and induced fluid circulation, but the extent of these hydrothermal systems is poorly known. Ar-Ar and fission track studies demonstrate widespread crustal cooling following extension (e.g., Miller et al., 1988; Snoko and Miller, 1988) as the geothermal gradient which was elevated by deformation relaxed back toward a normal range. Some combination of conduction and fluid flow would have removed the excess heat. Hydrothermal circulation in core complexes is clearly documented throughout the Basin and Range province, in Nevada, California, and Arizona (Lee et al., 1984; Kerrich and Rehrig, 1987; Roddy et al., 1988; Fricke et al., 1992); however, associated mass transfer into the brittle upper plate rocks of the extending crust has not been well studied. By the mid-Miocene, extension slowed and gave way to the development of Basin and Range-style, high-angle normal faults which are responsible for much of the current topography of the region (Zoback and Thompson, 1978; Thorman et al., 1991).

Characteristics of Carlin-Type Deposits

Carlin-type sediment-hosted gold deposits are widespread in the north-central portion of the Great Basin (Fig. 1), and reserve and production figures indicate an aggregate resource of over 100 million ounces (Moz) of gold (Dobra and Thomas, 1995). The general geologic characteristics of a number of these deposits have been tabulated by Tooker (1985), Bagby and Berger (1985), and Ilchik and Barton (1996). Data given in Ilchik and Barton (1996) are summarized in Table 1.

Carlin-type deposits are characterized by submicron-sized gold which is often present as inclusions in an isotopically distinctive epigenetic pyrite that contains 1 to 10 percent arsenic (Wells and Mullens, 1973; Arehart et al., 1993b). Gold is generally enriched between 100 to 1,000 times that present in unaltered host rocks. It is accompanied by an accessory suite of elements that includes arsenic, antimony, and commonly mercury, thallium, and/or silver. This suite is typically

TABLE 1. Characteristics of Carlin-Type Deposits

| | |
|-------------------------------|---|
| General features | |
| Metals | 0.1 to >30 Moz Au; increased As, Sb, Ba, \pm Hg, \pm Ag, \pm Tl ~100 times background; increased Pb, Zn, Cu <10 times background |
| Size (Mt) | <1 to >100 Mt at 0.5 ppm to ~15 ppm |
| Host rocks | Generally Pennsylvanian to Cambrian, silty to massive limestones and dolostones marl; Paleozoic mafic flows; hornfels; locally felsic dikes |
| Igneous and metamorphic rocks | Generally absent, when present Jurassic through Tertiary, intermediate to felsic; skarns are present near a few intrusions |
| Structure | Commonly at intersections of normal faults with favorable stratigraphy or thrust contacts |
| Alteration mineralogy | Carbonate dissolution and/or quartz deposition forming bedding and fault-controlled jasperoids and/or decarbonated zones; peripheral calcite veins and/or recrystallization of calcite or dolomite |
| Ore mineralogy | Quartz, illite, kaolinite, arsenical pyrite (2–6 wt % As), arsenopyrite, stibnite, realgar, orpiment, gold; postore barite \pm alunite, jarosite |
| Age | Mainly 40 to 20 Ma, other ages possible (e.g., Jurassic) |
| Conditions of formation | |
| T(°C) | Au ore stage 160 to 250, most between 190 and 225 |
| Pressure | 300 to 800 bars |
| Fluid compositions | Ore fluids 0 to 6 wt % NaCl equiv with significant CO ₂ and measurable H ₂ S; preore fluids up to 20 wt % NaCl equiv; stable isotopes (from fluid inclusions and calculated from silicates): $\delta D = -130$ to -155‰ ; $\delta^{18}O = -16$ to $+8\text{‰}$ |

See Ilchik and Barton (1996) for a summary of data for 16 major sediment-hosted deposits; other key references: Radtke et al. (1980), Holland et al. (1988), Bakken (1990), Ilchik (1990a), Kuehn and Rose (1992, 1995), Arehart et al. (1992, 1993b), Hofstra (1994)

enriched 100 times or more over background. In contrast, elements such as copper, lead, zinc, tungsten, bismuth, and tellurium rarely exceed 1 to 10 times background (e.g., Radtke et al., 1980; Ilchik, 1990a; Hofstra, 1994). Host rocks are generally organic matter-bearing, pyritic marls or massive limestones, but siliceous sedimentary rocks and mafic volcanic rocks locally host ore as well (cf. Raines et al., 1991). Alteration accompanying gold mineralization is characterized by the often complete removal of calcite and/or dolomite in the host rock and the addition of between 10 to greater than 90 wt percent quartz (Radtke et al., 1980; Bakken, 1990; Ilchik, 1990a; Kuehn and Rose, 1992; Hofstra, 1994). Textural information suggests that decalcification and/or silicification can be accompanied by significant volume loss as at Carlin (Bakken and Einaudi, 1986) or be nearly volume conservative as at Alligator Ridge (Ilchik, 1990a). Other significant constituents of ores include illite (generally inherited from a marly protolith), kaolinite (possibly inherited or as an alteration product of illite), and lesser amounts of diagenetic pyrite, epigenetic arsenian pyrite, arsenopyrite, realgar, orpiment, and stibnite. Peripheral to gold mineralization, host rocks remain calcareous and calcite veins abundant at the margin of the carbonate-leached, gold-bearing zones. Gold contents in these calcareous areas are generally several orders of magnitude below that found in adjacent decalcified zones. High-temperature, skarn-type alteration is present only where de-

posits adjoin intrusive rocks, but geologic data indicate that igneous activity predated gold mineralization (Ilchik, 1995; but for an alternative interpretation see Arehart, 1993a). Among sulfates, barite is a common late vein mineral, whereas alunite and jarosite, although widespread, appear related to weathering (Arehart et al., 1992).

Orebodies range in size from less than 1 Mt to more than 100 Mt (Ilchik and Barton, 1996). Mineralization is generally localized near fault intersections with favored lithologies. Within districts multiple orebodies typically occur in similar settings. Despite the large extent of many districts, studies to date have not identified district-scale zoning patterns for alteration, metal ratios, or fluid inclusion temperatures (Tooker, 1985; Raines et al., 1991; Ilchik, unpub. data, 1995). Regional controls on the distribution of mineralization are unclear, but many deposits are crudely aligned along trends which may be up to 150 km in length (Fig. 1; Roberts, 1966; Roberts et al., 1971; Cunningham, 1988; Raines et al., 1991; Maher et al., 1993). These trends may indicate regional-scale controls on fluid circulation and mineralization such as the amount and orientation of mid-Tertiary extension (see discussion in Seedorff, 1991). Alternatively, some trends may represent selective exposure.

Many Carlin-type deposits occur away from known igneous centers (Table 1; Tooker, 1985; Raines et al., 1991), whereas others are near Mesozoic and/or Cenozoic intrusive centers (Getchell, Gold Acres, Bald Mountain, and Goldstrike). At most of these deposits there is evidence for postintrusion disturbance of K-Ar systematics of the igneous rocks, an indication that these rocks predate gold mineralization (Silberman et al., 1974; Ilchik, 1995; Ilchik and Barton, 1996). Furthermore, metal and alteration zoning patterns associated with gold mineralization do not indicate a systematic relationship to a central intrusive body (Willden, 1964; Silberman et al., 1974; Wrucke and Armbrustermacher, 1975). More commonly, deposits are devoid of igneous rocks or have at most widely scattered dikes and volcanic rocks that are typical of the region (Alligator Ridge, Ilchik, 1990a; Jerritt Canyon, Daly et al., 1991).

Fluid inclusion and stable isotope data from a number of localities indicate the deposits formed at relatively cool temperatures under moderate pressures from dilute meteoric waters that have exchanged isotopically with sedimentary rocks prior to gold deposition. Data from three-phase ($L_{H_2O} + L_{CO_2} + V_{CO_2}$) fluid inclusions indicate that temperatures were generally between 175° and 225°C and that the pressures were most likely between 400 and 1,500 bars (Cline et al., 1993; Lamb and Cline, 1993; Kuehn and Rose, 1995). These inclusions also indicate that ore fluids were generally low salinity (<5 wt % NaCl equiv). Hydrogen isotope data from both fluid inclusions and hydrous alteration phases show that the ore fluids were light ($\delta D_{H_2O} < -100\text{‰}$; Rye et al., 1974; Radtke et al., 1980; Ilchik, 1990b; Hofstra, 1994) and thus likely to be derived from Late Cretaceous or Tertiary meteoric water. Oxygen isotope data indicate that ore fluids were heavier than meteoric water (-10 to +4‰) and suggest an involved interaction with sedimentary rock prior to gold deposition (Rye, 1985; Hofstra et al., 1988; Holland et al., 1988; Ilchik, 1990a). Sulfur isotopes from epigenetic sulfides

are heavy (5–25‰; Radtke et al., 1980; Ilchik, 1990a; Arehart et al., 1993b; Hofstra, 1994) and are compatible with a sedimentary source for sulfur. Conversely, these data are inconsistent with an igneous source for the same components.

The age of formation of these deposits is controversial; interpretation is complicated by the general lack of datable hydrothermal minerals. Proposed ages range from Jurassic to Miocene, but we know of no example where rocks of pre-mid-Tertiary age crosscut Carlin-type gold mineralization or related alteration. Maximum ages in many cases are provided only by the mid- to late Paleozoic ages of the youngest host rocks. In some deposits, mineralization crosscuts Jurassic or Cretaceous stocks (e.g., Getchell, Post-Betze, Gold Acres). Late Eocene-early Oligocene felsic dikes or tuffs at Carlin, Goldstrike, Jerritt Canyon, Getchell, and Cortez are hydrothermally altered and indicate a mid-Tertiary or younger age (Bakken and Einaudi, 1986; Maher et al., 1993; Ilchik, 1995; Phinisey, 1995; but see Arehart et al., 1993a, for an alternative interpretation). A mid-Tertiary origin is also consistent with the localization of deposits along Cenozoic normal faults (Seedorff, 1991). Radiometric ages on post-main-stage alunite (usually middle to late Miocene, Ilchik, 1990a; Arehart et al., 1992), pressure estimates from fluid inclusions which indicate formation at or near maximum burial depths, and crosscutting relationships between mineralization and Basin and Range high-angle faulting (e.g., Getchell, Joralemon, 1951; Alligator Ridge, Ilchik, 1990a; Genesis deposit, Paul et al., 1993) all indicate that mineralization predates late Miocene Basin and Range uplift. Thus, the accumulated evidence is consistent with mineralization taking place during mid-Tertiary extension followed by uplift in the Miocene.

Models of Possible Origin

Carlin-type systems have been interpreted in terms of three modes of origin: igneous related (circulation of magmatic or external fluids by igneous activity), metamorphic (release of fluid during regional thermal metamorphism), or amagmatic (circulation of nonmagmatic fluids during regional extension). Any viable model must ultimately rationalize both deposit-scale characteristics and the broader relationships to regional geology and tectonism. At deposit scales, addition of gold and quartz, the removal of carbonate, the absence of base metals, and evidence for a relatively low-temperature, dilute meteoric fluid are key observations. Features which require explanation at the regional scale include the apparent restriction to the Cordilleran miogeocline, the lack of close association with igneous rocks, the permissive association with mid-Tertiary extension, and the lack of district-scale zoning.

Igneous-related origin

A spatial association of some Carlin-type deposits with Mesozoic intrusive centers (e.g., Getchell, Gold Acres, Goldstrike, and Bald Mountain) and the genetic link of some types of gold ores with intrusive events has led to the interpretation that Carlin-type deposits are distal portions of magmatic hydrothermal systems (Radtke et al., 1980; Alvarez and Noble, 1988; Sillitoe and Bonham, 1990; Arehart et al., 1993a). This model proposes a direct link to igneous activity since magmas provide the energy to drive hydrothermal circulation as well as providing the fluids and their minor constituents including

gold. This hypothesis, however, is not compelling for several reasons. As noted above, Carlin-type deposits lack demonstrable time-space links to intrusive centers. Neither do they show district-scale temperature or geochemical zoning features like those found in many porphyry-related precious metal deposits (Sillitoe, 1988). The lack of nearby enrichments in base metals or silver contrasts with districts where gold-bearing jasperoids have igneous connections (e.g., Purísima Concepción, Peru, Alvarez and Noble, 1988; Leadville, Colorado, Beatty et al., 1990; Ely, Nevada, Maher, 1996). Furthermore, isotopic data preclude a large magmatic component, but instead indicate a predominantly sedimentary source for sulfur and a meteoric one for H₂O. Likewise, Carlin-type deposits differ from volcanic-hosted epithermal gold systems in their styles, types of alteration assemblages, and formation at higher pressures and lower temperatures (Table 1). Nothing precludes igneous-driven circulation of meteoric fluids through the sedimentary section (as suggested by Radtke et al., 1980) in districts with contemporaneous magmatism, provided that similar fluid compositions and alteration are generated. Nevertheless, the regional pattern of deposits implies broad hydrologic systems, one that is inconsistent with the more restricted distribution of known intrusive centers in the region.

Regional metamorphic origin

Models invoking a regional metamorphic origin suggest that deep-seated, possibly mantle-derived magmatic activity preceded crustal extension and provided sufficient heat to generate and circulate the fluids required for deposit formation (Seedorff, 1991). This model suggests that H₂O and CO₂ in the hydrothermal fluid were derived from devolatilization reactions of subjacent metasedimentary rocks, with metals and sulfur being scavenged from this source as well. Igneous heat may be involved, but only in a regional sense. Derivation of sufficient H₂O from dehydration reactions to account for the known mineralization and the light δD values of the ore fluids, as noted by Seedorff (1991), are major problems for this model. A further difficulty is the absence of compelling evidence for mid-Tertiary regional metamorphism, the thermochronology generally indicating a Late Cretaceous thermal maximum with perhaps only a rapid cooling in the mid-Tertiary (e.g., Miller et al., 1987).

Amagmatic origin—fluid circulation during crustal extension

An amagmatic model for the genesis of Carlin-type deposits suggests that the hydrothermal systems were a result of thermal and permeability anomalies created during mid-Tertiary extension in the Basin and Range province (Ilchik, 1990b). Although the details of extension are complex, the general characteristics are well established (e.g., Dickinson, 1991). By systematically bringing hotter, more deeply buried rocks toward the surface, crustal thinning must raise the geothermal gradient (Fig. 2). Brittle faulting in the upper 10 km of the crust increases secondary permeability. Consequently, by increasing the temperature gradient, the permeability, and possibly, the topographic relief, the likelihood of fluid circulation is greatly enhanced (e.g., section 9-9 in Turcotte and Schubert, 1982). Synextensional penetration of meteoric water to

the brittle-ductile transition of metamorphic core complexes of eastern Nevada is amply indicated by isotopic data (e.g., Lee et al., 1984; Fricke et al., 1992; M.D. Barton and R.P. Ilchik, unpub. data, 1988). Deep circulation of meteoric water leads to reaction with the variably reduced sedimentary rocks of the miogeocline resulting in dilute silica- and sulfide-bearing solutions capable of scavenging gold but not base metals. New and rejuvenated structures serve to localize flow during fluid ascent. Along the ascent paths various mechanisms including cooling, decompression, mixing, and wall-rock reaction might under appropriate circumstances lead to Carlin-type mineralization.

Tests of these models

To assess this extension-driven model for Carlin-type mineralization, we first compare the energy balance for the various genetic models and attempt to place limits on the masses of fluids which these processes might circulate. We then model mass transfer for multiple combinations of possible source rocks and depositional processes.

Physical Constraints on Hydrothermal Circulation

A constraint of any genetic mechanism is the ability to circulate sufficient hot water (>200°C) to form appropriate volumes of alteration. The results of simple calculations of heat balance for both amagmatic and magmatic cases are illustrated in Figure 3. Ample heat is available in extended upper crust if it can be extracted efficiently. Likewise, moderate volumes of magma contain comparable heat. Hydrothermal convection driven by magmatic heat has been widely examined (e.g., Cathles, 1981; Norton, 1982; Hanson, 1995), but less attention has been paid to limits on hydrothermal flow driven by extension (cf. Buck et al., 1988; Pearson and Garven, 1994). We estimate the heat balance in both cases using simple geometries and assuming linear geotherms (Figs. 2 and 3).

In the case of magmatism, an upper bound on available heat reflects the temperature of the intrusion in excess of the geotherm. A few to a few tens of volume percent intrusion provides approximately 10¹⁸ to 10¹⁹ J/km² (Fig. 3). As numerous numerical studies have shown, this heat is shed rapidly, with a significant portion partitioned into hydrothermal systems when permeabilities are greater than about 1 mD (10⁻¹⁵ m²; e.g., Hanson, 1995).

For extension, if the process is rapid compared to times needed for conductive cooling of the upper crust (i.e., <3–10 m.y.; as it probably was in any given area in the Great Basin, see figs. 5, 6, 7 in Seedorff, 1991), then the geotherm initially rises in proportion to the amount of extension. An estimate of the heat available to hydrothermal systems can be derived by comparing geotherms before and immediately after rapid extension (Fig. 2). The amount of heat, H^o, contained in a unit surface area column of crust prior to extension is:

$$H^o = \frac{A^o \cdot h^o{}^2 \cdot \rho \cdot C_{pr}}{2}, \quad (1)$$

where h^o, ρ , and C_{pr} are the thickness, density and heat capacity of the crust and A^o is the initial geotherm. Following

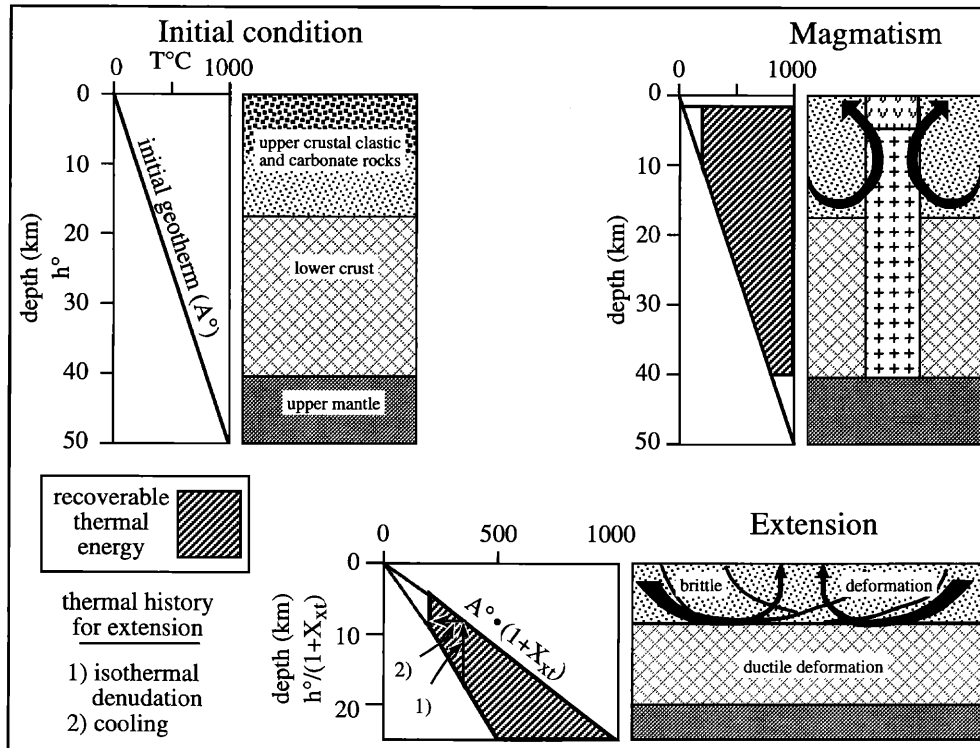


FIG. 2. Comparison of extension and magmatism as energy sources to drive hydrothermal circulation. Rapid lateral extension thins the crust and raises the initial geothermal gradient, A° , proportional to the amount of extension $(1 + X_{xt})$. If the geothermal gradient returns to its initial value after extension ceases, then the amount of heat potentially available to drive hydrothermal circulation is shown by the crosshatched area. Release of this heat results in cooling of the crust, as indicated by the thermal path for rocks initially at 300°C . A magmatic example where a column of magma is intruded at $1,000^\circ\text{C}$ and extends from the base of the crust to the surface is shown for comparison. Ten volume percent intrusion and 100 percent extension release roughly equal amounts of heat. For extension, this energy and the resultant circulation would be evenly distributed across the surface. For magmatism, however, heat and circulation would be centered on individual intrusions. See text for explanation of symbols.

extension and assuming constant volume, the thickness of the column is $h^\circ/(1 + X_{xt})$ and the geotherm is $A^\circ \cdot (1 + X_{xt})$, where X_{xt} is the fractional amount of horizontal extension. By analogy with (1), if we assume that the geotherm relaxes to its original value due to limits on the input of new heat from radioactive decay and the mantle, then the amount of heat in a postextension unit area column of crust, H^f , is:

$$H^f = \frac{A^\circ \cdot [h^\circ/(1 + X_{xt})]^2 \cdot \rho \cdot C_{pr}}{2} \quad (2)$$

The heat released by extension following thermal relaxation, H_{xs} , is approximately the difference between H° and H^f and normalized to postextension surface area, is:

$$H_{xs} \approx \frac{A^\circ \cdot \left\{ h^{\circ 2} - (1 + X_{xt}) \cdot \left[\frac{h^\circ}{1 + X_{xt}} \right]^2 \right\} \cdot \rho \cdot C_{pr}}{2 \cdot (1 + X_{xt})} \quad (3)$$

Comparisons between extension and magmatism show that a 20 percent extension of a 40-km-thick lithosphere with an initial geotherm of $20^\circ\text{C}/\text{km}$ releases approximately the same amount of heat as the cooling of a 10 vol percent intrusion ($\sim 7 \times 10^{18} \text{ J}/\text{km}^2$), and that 100 percent extension releases

the heat equivalent of just under a 20 vol percent intrusion ($1.1 \times 10^{19} \text{ J}/\text{km}^2$; Fig. 3).

Extension also promotes convective fluid flow by increasing permeabilities through faulting, fracturing, and brecciation. Permeabilities need only be a few millidarcies for thermal convection to take place on the length scales (5–10 km) and thermal gradients (10° – $40^\circ\text{C}/\text{km}$) appropriate to extended crust of the Basin and Range (e.g., see Turcotte and Schubert, 1982, p. 405). Thus, once extension begins and permeability is enhanced, rapid dissipation of heat through convection should occur. Only after the geothermal gradient is diminished or permeability is occluded (for example, by reaction) would circulation cease. Present-day amagmatic fault-controlled geothermal systems in the Great Basin may be modern analogues.

In both the magmatic and amagmatic cases, the amount of fluid potentially circulated to dissipate excess heat is roughly:

$$M_f \approx \frac{H_{xs}}{(C_{pf} \cdot \Delta T)}, \quad (4)$$

where M_f is the mass of fluid, ΔT is the temperature change of the fluid, and C_{pf} is the average heat capacity of the fluid. For the estimates shown in Figure 3, we assume a ΔT of

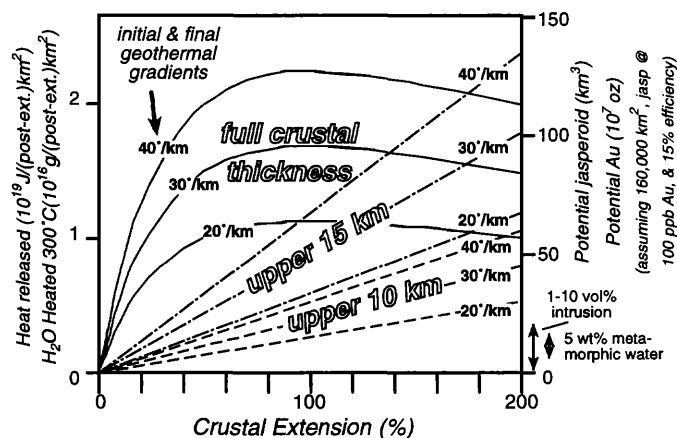


FIG. 3. Relationship between amount of crustal extension, thermal energy for hydrothermal circulation, and gold resource potential of the east-central Great Basin ($\sim 160,000 \text{ km}^2$). Three models for heat released are based on amount of crust involved and initial geotherm. Solid lines = total initial crust to 40 km, dash-dot line = upper 15 km after extension, and dashed line = upper 10 km after extension. Amount of heat released in the full crustal model has a maximum at 100 percent extension due to interplay between the mass of crust involved, which decreases as the amount of extension increases, and the linear increase in the geotherm with extension. Other models are linear because the initial thickness of crust increases as the amount of extension increases. The amount of potential jasperoid is limited by the transport of 0.5 g of SiO_2 per kg of fluid and a 15 percent efficiency for process; the amount of gold assumes an average grade of 100 ppb. The amounts of jasperoid and gold which could be transported and deposited by an igneous-driven system or one utilizing metamorphic water are shown for comparison.

325°C , based on circulation down to the brittle-ductile transition (as shown in core complexes; Kerrich and Rehrig, 1987; Fricke et al., 1992). Although greater masses of water would be heated for a lower ΔT , ore formation requires moderate temperatures.

Heat balance considerations indicate that the mass of water that can be circulated by crustal extension is large (Fig. 3). Regionally, it may significantly exceed the mass that can be circulated by igneous-driven convection or released from plausible pore fluids or metamorphic reactions. Figure 3 also shows the amount of water potentially circulated by 1 to 10 vol percent intrusion, and the pore/metamorphic water inventory to a 15-km depth of crust assuming 5 wt percent water. In this simple analysis, extension can easily heat enough water to account for the volume of known and suspected mineralization, even if only at 15 percent efficiency (right-hand side scales, Fig. 3). In contrast, igneous-driven and metamorphic waters are only roughly adequate with high efficiencies. Thus, given more-than-sufficient energy sources and a plausible fit with geologic constraints, the chemical efficacy of amagmatic fluids in extracting, transporting, and depositing the components of Carlin-type deposits becomes the central issue.

The initial and final conditions that we impose in these calculations (i.e., return of the geotherm to its preextension value, and thus a transient increase in heat flow) represent one of many possible scenarios. Regardless of the final thermal gradient, convection commences in response to extension-caused increase of the geotherm and permeability. Our

choice of conditions simplifies estimation of the energy available to drive circulation; by assuming a transient event and no other heat input, it represents a plausible minimum.

Source to Deposit Geochemical Modeling of Carlin-Type Systems

To assess the geochemical viability of the amagmatic model, we simulated mass transfer due to hydrothermal circulation within a crustal column like that of the Great Basin using numerical methods based on equilibrium thermodynamics (Helgeson, 1979; Frantz et al., 1981). Simulations are based on a two-step, source to deposit approach. They explore cooling, wall-rock alteration, and fluid mixing as mechanisms for ore deposition (Fig. 4). In the simulations, a source fluid composition is calculated assuming equilibrium with plausible (meta)sedimentary mineral assemblages at appropriate conditions of temperature, pressure, ΣCl , and $\pm X_{\text{CO}_2}$. This fluid is then reequilibrated under various conditions that simulate potential depositional settings. Mass transfer between source and deposit is estimated as the difference between aqueous concentrations of the various components in the source-rock-equilibrated and deposit-equilibrated fluids. The approach allows a systematic examination of many sources and depositional mechanisms.

The source calculations provide an independent constraint on the nature of potential ore-forming fluids and can be directly compared with estimates from deposit studies and measured metal-bearing fluids. Although the simulations address Au-dominated, base metal-poor deposits, the incorporation of Zn and Pb provides insight into a spectrum of ore-forming processes. Metal mobilities vary greatly with source-rock compositions and ΣCl . Similar diversity at the deposit level indicates the breadth of possible alteration types and metal contents.

Method of calculation

Fluid-rock equilibria were calculated from a system of mass action and mass balance equations using the computational approach of Frantz et al. (1981) based on the method of Van Zeggeren and Storey (1970). Simultaneous solution of the mass action equations, representing the dissolution of minerals and dissociation of aqueous complexes, and the mass balance equations, representing additional constraints on bulk compositions (e.g., ΣCl , charge balance), was done by an iterative matrix inversion method. It was considered that mineral phases were present in excess and that incremental amounts of fluid were reacted with the solid assemblage. Thus, at any particular stage of reaction, the system is rock dominated, but summation of incremental mass transfer predicts results at increasing water to rock ratios. Criteria for convergence on a solution to the system of equations was a change of less than one part per 10,000 for each species considered.

The thermodynamic components of the system consisted of SiO_2 , Al_2O_3 , CaO , MgO , FeO , Na_2O , K_2O , H_2O , CO_2 , H_2SO_4 , H_2S , H^+ , Cl^- , Au, Pb, and Zn. Aqueous activities and concentrations were calculated for 39 ions and complexes listed in Table 2. Equilibrium constants for all mass action equations were taken from SUPCRT92 (Johnson et al., 1992) with the exception of those involving gold (Seward, 1973;

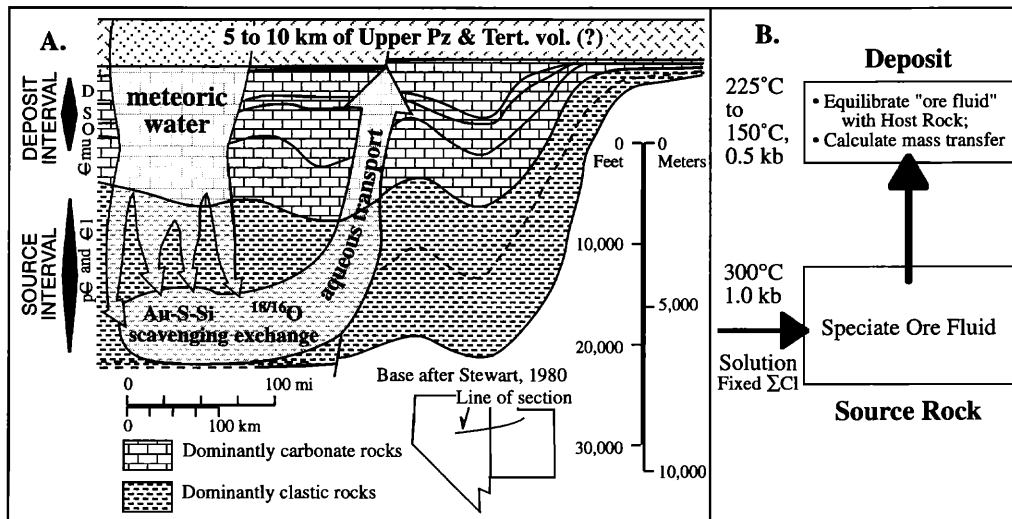


FIG. 4. A. Diagrammatic fluid circulation model for the formation of Carlin-type deposits shown on a stratigraphic section for the east-central Great Basin. During regional extension, Early to mid-Tertiary meteoric waters circulate to near the brittle-ductile transition where sulfur, gold, and silica are leached from clastic sediments. Heated, buoyant fluids are channeled into faults. At the deposit level, fluids spread into permeable horizons, leach carbonate, and deposit gold and silica. "P2 + Tert. vol." = additional Paleozoic and Tertiary volcanic cover at time of deposit formation. B. Schematic overview of geochemical modeling procedure. Fluid with a fixed ΣCl is first equilibrated with a potential source rock. This fluid is then reequilibrated under various conditions representative of the deposit environment. Mass transfer is estimated from the difference between fluid compositions in the two environments.

Shenberger and Barnes, 1989; Hayashi and Ohmoto, 1991) and HCl° (Sverjensky et al., 1991). The SUPCRT92 database does not include data for As- and Sb-bearing species, thus these species were not included in the calculations. Activity coefficients for charged aqueous species are from Helgeson et al. (1981) and Reed and Spycher (1990). Equilibrium constants for the aqueous gold species are from Shenberger and Barnes (1989; along the liquid-vapor H_2O curve) and from Seward (1973; at 1 kbar); data for $\text{HAu}(\text{HS})_2^\circ$ are from Hayashi and Ohmoto (1991). Pressure corrections for the solubility of gold as $\text{Au}(\text{HS})_2^\circ$ were obtained by linear interpolation between the pressures used in the two sets of experiments.

Several simplifying assumptions were used in this study. The calculated mass transfer assumes that the fluid composi-

tion is unchanged between the source and deposit. The activity of water is fixed at unity throughout, and CO_2 in the aqueous fluid is assumed to follow the behavior of Henry's law. Biotite and chlorite were treated as ideal site solutions of annite-phlogopite and daphnite-clinocllore, respectively. Metal concentrations in solution were calculated assuming equilibrium with the native gold, sphalerite, and galena, thus the calculations represent maximum concentrations. Reaction kinetics were not treated, although we considered the implications of disequilibrium among C-O-H-S species.

It is difficult to assess fully uncertainties in these calculations. Uncertainties in most thermodynamic data are on the order of a few kJ/mole, thus uncertainties (which can be highly correlated) in equilibrium constants are generally <1 log unit, in some cases as little as 0.1 log unit (Johnson et al., 1992; Nordstrom and Munoz, 1994). Experimental data on gold solubilities suggest that the uncertainty in $\log K$ for $\text{Au}(\text{HS})_2^\circ$ may be as high as ± 0.5 log units (Benning and Seward, 1996). Consequently, these calculations should be viewed for their qualitative insight into the effects of various geologic processes on gold transport and deposition and not as accurate estimates of mass transfer. In the following sections we present a synopsis of the numerical results; a full set of computational results is available from the senior author upon request.

Source-Rock Calculations

Conditions

Fluid-source rock equilibria were simulated at 300°C and 1.0 kbar using a variety of mineral assemblage lithologies that represent arkoses, graywackes, and pelites (Table 3). Total chloride was varied from 0.1 to 1.0 m , in ~ 0.3 - m increments, for all model lithologies and f_{O_2} and f_{S_2} buffers. Mineralogy

TABLE 2. Species Used in Calculation of Fluid/Mineral Equilibria

| Element and species | Reference |
|---|-----------|
| Na: Na^+ , NaCl° | 1 |
| K: K^+ , KCl° , KSO_4^- | 1 |
| Ca: Ca^{2+} , CaCl^+ , CaCl_2° , CaHCO_3^+ | 1 |
| Mg: Mg^{2+} , MgCl^+ , MgHCO_3^+ | 1 |
| Fe: Fe^{3+} , FeCl^+ | 1 |
| H: H^+ , OH^- | 1 |
| Si: $\text{H}_4\text{SiO}_4^\circ$ | 1 |
| Cl: Cl^- , HCl° | 1, 2 |
| S: SO_4^{2-} , HSO_4^- , HS^- , H_2S° | 1 |
| C: $\text{H}_2\text{CO}_3^\circ$, HCO_3^- , CH_4 | 1 |
| Pb: Pb^{2+} , PbCl^+ , PbCl_2° , PbCl_3^- , PbCl_4^{2-} | 1 |
| Zn: Zn^{2+} , ZnCl^+ , ZnCl_2° | 1 |
| Au: $\text{Au}(\text{HS})_2^\circ$, $\text{HAu}(\text{HS})_2^\circ$ | 3, 4, 5 |

References: (1) Johnson et al. (1992), (2) Sverjensky et al. (1991), (3) Shenberger and Barnes (1989), (4) Seward (1973), (4) Hayashi and Ohmoto (1991)

TABLE 3. Source Rock Mineralogies

| Arkose | Graywacke | Pelite |
|---|--|--|
| Present in all runs: | | |
| Gold | Gold | Gold |
| Quartz | Quartz | Quartz |
| Low albite | Paragonite | Paragonite |
| K feldspar | Margarite | Margarite |
| Muscovite | Muscovite | Muscovite |
| Clinozoisite | Clinozoisite | Kaolinite |
| Galena | Galena | Galena |
| Sphalerite | Sphalerite | Sphalerite |
| Phlogopite ¹ | Clinoclhore ¹ | Clinoclhore ¹ |
| Pyrite | Pyrite | Pyrite |
| Magnetite + hematite or pyrrhotite ² + annite (X _{Fe} = 0.65, 0.48, 0.37) | Magnetite + hematite or magnetite + pyrrhotite ² or pyrrhotite ² + daphnite (X _{Fe} = 0.49, 0.37, 0.27) | Magnetite + hematite or magnetite + daphnite (X _{Fe} = 0.71) or pyrrhotite ² + daphnite (X _{Fe} = 0.58, 0.43, 0.33) |
| Calcite or f _{CO₂} fixed at 10 bars | Calcite or calcite or graphite | Calcite or calcite or graphite |
| Total chlorinity: fixed at 1.0, 0.67, 0.33 or 0.1 m | | |

¹ Activity adjusted to correspond with f_{O₂} and f_{S₂} buffers

² Activity = 0.6

and ΣCl served to buffer pH (Fig. 5). Combinations of Fe-S-Si-O minerals ± graphite-CO₂ equilibria were used to buffer f_{O₂} and f_{S₂} (Table 3, Fig. 6). These model mineral assemblages span much of the natural compositional variation for low-grade metasedimentary lithologies and are broadly consistent with the terrigenous detrital succession thought to be a basement lithology throughout much of the northeastern Great Basin (cf. Misch and Hazzard, 1962). The variation in

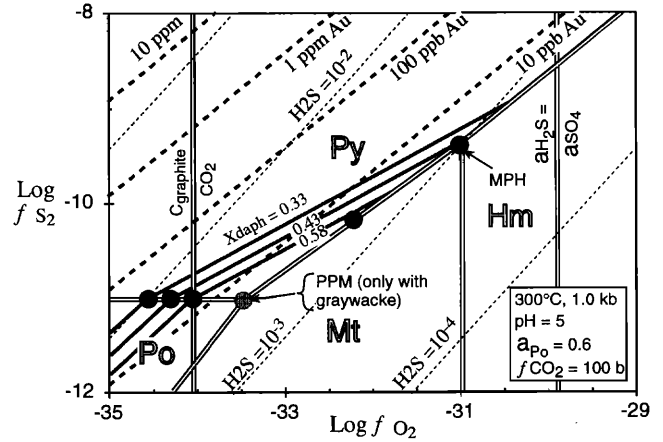


FIG. 6. Mineralogical buffers used to fix f_{O₂} and f_{S₂} for source conditions (dots; only pelite assemblage shown for simplicity). Decreasing the iron content of chlorite (X, heavy solid lines) along pyrite-pyrrhotite increases the activity of aqueous sulfur (light dashed lines), and hence gold concentrations (as Au(HS)₂; heavy dashed lines). The reaction determining chlorite solid solution is daphnite + 5S₂ = pyrite + kaolinite + quartz + 2.5O₂ + 23H₂O; ideal site mixing was assumed (a_{daphnite} = (X_{Fe^{chlorite}})⁵). Compositions of chlorites and biotites used for graywacke and arkose assemblages, respectively, are given in Table 3.

calculated fluid compositions due to the varied source assemblages is considerably greater than the uncertainties due to errors in the thermodynamic data. In total, over 100 combinations of the mineral assemblages with differing carbon and f_{O₂} - f_{S₂} buffers and ΣCl were evaluated.

Results

Gold: Calculated aqueous gold concentrations for source-rock-equilibrated fluids vary from 0.7 to 300 ppb (Fig. 7A, Table 4). Low-chlorinity fluids equilibrated with pyrite-pyrrhotite-annite-bearing arkosic assemblages had the greatest gold contents, whereas high-chlorinity fluids from the magnetite-bearing pelitic assemblages had the lowest gold contents. The Au(HS)₂ complex accounted for 95 to 99 percent aque-

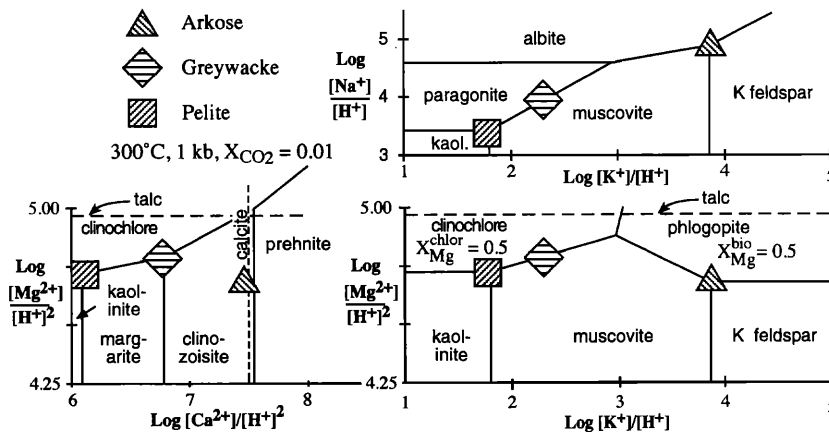


FIG. 5. Activity-activity diagrams for source conditions (300°C and 1 kbar) showing mineral assemblages for the three source lithologies considered. A key variation is the decrease in the cation/hydrogen ion ratio from arkose to pelite. At any ΣCl, this produces a decrease in pH of about 1 log unit, which in turn, strongly affects aqueous metal concentrations and ratios in solution (cf. Fig. 7C).

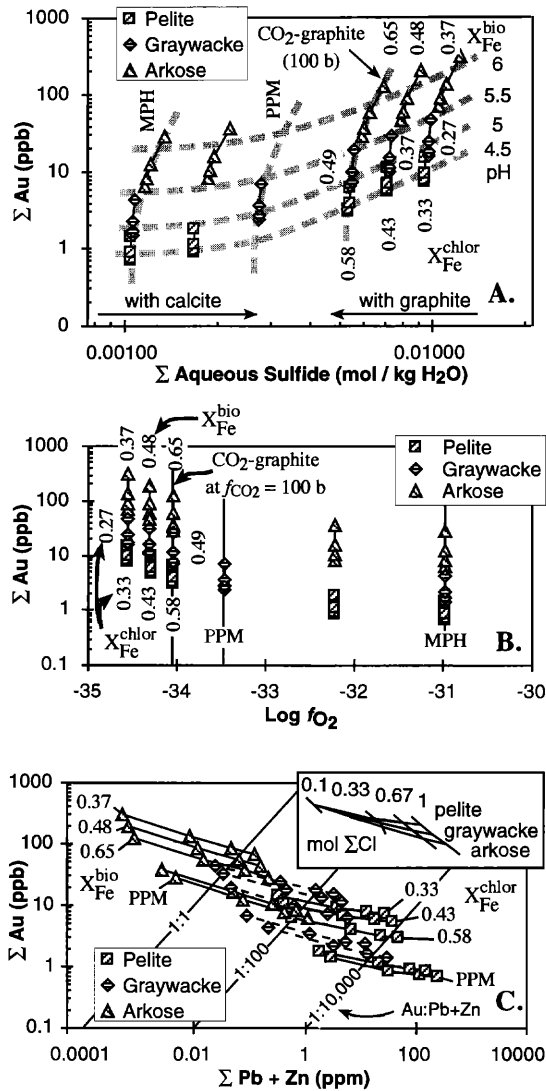


FIG. 7. Results of selected source calculations (300°C and 1 kbar) showing effects of lithology, $f_{O_2} - f_{S_2}$ buffers, and chlorinity (varied from 1.0 to 0.1 m) on metal solubility. Symbols denote lithology; thin solid lines connect groups calculated at constant f_{O_2} , f_{S_2} buffers (i.e., X_{Fe}^{bio}), but with variable ΣCl ; iron contents of phyllosilicates and a ΣCl (heavy dashed lines) are indicated where space permits. A. Aqueous gold vs. reduced sulfur concentrations. Gold solubility decreases and pH increases for any particular lithology and $f_{O_2} - f_{S_2}$ buffer as ΣCl increases from 0.1 to 1.0 molal. Abbreviations: PPM = pyrrhotite-pyrite-magnetite, MPH = magnetite-pyrite-hematite. B. Aqueous gold concentration vs. f_{O_2} . If changes in ΣS are not considered, gold solubility should decrease with decreasing f_{O_2} . However, increases in aqueous ΣS as the source rocks becomes increasingly reduced overrides decreasing f_{O_2} (cf. Fig. 6). C. Base metal vs. gold solubility. ΣCl increases and pH decreases for a given lithology and oxidation state toward the right, hence acid, high chloride fluids favor base metal transport, whereas neutral, lower chlorinity fluids favor gold.

ous gold in arkose-equilibrated fluids, and 60 to 80 percent in fluids from pelitic assemblages. The maximum calculated concentration for $H Au(HS)_2^-$ was 3.0 ppb. Changes in $\Sigma S_{reduced}$, mineralogy, and ΣCl (the latter two through effects on pH) account for roughly equal amounts of the variation in aqueous gold concentrations. The relative unimportance of f_{O_2} directly on gold concentrations is shown by the decrease

TABLE 4. Comparison of Calculated Fluids with Measured Data for Carlin-Type Deposits and Some Epithermal Systems

| T°C | pH (@T) | Cl (ppm) | H ₂ S (ppm) | SO ₄ (ppm) | CO ₂ (ppm) | CH ₄ (aq) (ppm) | SiO ₂ (ppm) | Na (ppm) | K (ppm) | Ca (ppm) | Fe (ppm) | Zn (ppm) | Pb (ppm) | Au (ppb) | This study | | | | | |
|-----|-------------------------|--------------------|-------------------------|-------------------------|-----------------------|----------------------------|-------------------------|----------------------|----------------------|-------------------------|----------------------|----------------------|-------------------------|------------------|--------------------------------|--------------------------------|-----------------------------|-----------------------------|-----------------------------|--------------------------------------|
| | | | | | | | | | | | | | | | Maximum (assemblage indicated) | Minimum (assemblage indicated) | Typical arkose ¹ | Typical pelite ² | Carlin deposit ³ | Jerritt Canyon district ⁴ |
| 300 | 6.2 ^a | 35,400 | 390 ^a | 170 ^a | 130,000 ^b | 3,610 ^c | 800 ^a | 19,960 ^a | 2,900 ^a | 9,700 ^a | 33 ^a | 190 ^a | 60 ^a | 302 ^a | 300 | 215 ± 30 | 225 | 300 | 250-350 | 250 |
| | 4.3 ^b | 3,540 | 35 ^{b,p} | 1.8 · 10 ^{-7p} | 4,000 ^a | 0 ^a | 800 ^b | 2,020 ^b | 80 ^b | 15 ^a | 0.00045 ^a | 0.00047 ^a | 3.3 · 10 ^{-5a} | 0.7 ^a | 11,700 | 12,000-25,000 | 35,400 | 6,000-30,000 | 32,000-66,000 | |
| | 3.5 ^{b,p} | 390 ^a | 170 ^a | 130,000 ^b | 3,610 ^c | 800 ^a | 19,960 ^a | 2,900 ^a | 9,700 ^a | 33 ^a | 190 ^a | 60 ^a | 302 ^a | 300 | 1,620 | 1,080 | 1,080 | 6,000-30,000 | 5-250 | |
| | 1.8 · 10 ^{-7p} | 4,000 ^a | 0 ^a | 800 ^b | 2,020 ^b | 80 ^b | 15 ^a | 0.00045 ^a | 0.00047 ^a | 3.3 · 10 ^{-5a} | 0.7 ^a | 11,700 | 12,000-25,000 | 35,400 | ND | 1,620 | 3,200 | 190 | ND | |
| | 0 ^a | 800 ^b | 1.8 · 10 ^{-7p} | 4,000 ^a | 3,610 ^c | 800 ^a | 19,960 ^a | 2,900 ^a | 9,700 ^a | 33 ^a | 190 ^a | 60 ^a | 302 ^a | 300 | ND | ND | 1.6 · 10 ⁻⁵ | 10 | 950-1,900 | |
| | 800 ^b | 2,020 ^b | 80 ^b | 15 ^a | 0.00045 ^a | 0.00047 ^a | 3.3 · 10 ^{-5a} | 0.7 ^a | 11,700 | 12,000-25,000 | 35,400 | 3,200 | 1,080 | 300 | 100,000-200,000 | 100,000-200,000 | 88,000 | 10,800 | 100,000-300,000 | |
| | 9,700 ^a | 33 ^a | 190 ^a | 60 ^a | 302 ^a | 300 | 215 ± 30 | 225 | 300 | 250-350 | 250 | 300 | 215 ± 30 | 225 | 1,450 | 8,000-15,000 | 240 | 500 | ND | |
| | 33 ^a | 190 ^a | 60 ^a | 302 ^a | 300 | 215 ± 30 | 225 | 300 | 250-350 | 250 | 300 | 215 ± 30 | 225 | 300 | 8,000-15,000 | 8,000-15,000 | 23,000 | 640 | 4,000-20,000 | |
| | 190 ^a | 60 ^a | 302 ^a | 300 | 215 ± 30 | 225 | 300 | 250-350 | 250 | 300 | 250 | 300 | 215 ± 30 | 225 | 1,450 | 1,450 | 670 | 145 | 19,000-38,500 | |
| | 60 ^a | 302 ^a | 300 | 215 ± 30 | 225 | 300 | 250-350 | 250 | 300 | 250 | 300 | 215 ± 30 | 225 | 300 | 8,000-15,000 | 8,000-15,000 | 670 | 0.6 | 3,500-7,300 | |
| | 302 ^a | 300 | 215 ± 30 | 225 | 300 | 250-350 | 250 | 300 | 250 | 300 | 250 | 300 | 215 ± 30 | 225 | 1,450 | 1,450 | 80 | 0.6 | ND | |
| | 300 | 215 ± 30 | 225 | 300 | 250-350 | 250 | 300 | 250 | 300 | 250 | 300 | 215 ± 30 | 225 | 300 | 8,000-15,000 | 8,000-15,000 | 80 | 0.6 | ND | |
| | 215 ± 30 | 225 | 300 | 250-350 | 250 | 300 | 250 | 300 | 250 | 300 | 250 | 300 | 215 ± 30 | 225 | 1,450 | 1,450 | 80 | 0.6 | ND | |
| | 225 | 300 | 250-350 | 250 | 300 | 250 | 300 | 250 | 300 | 250 | 300 | 215 ± 30 | 225 | 300 | 8,000-15,000 | 8,000-15,000 | 80 | 0.6 | ND | |
| | 300 | 250-350 | 250 | 300 | 250 | 300 | 250 | 300 | 250 | 300 | 250 | 300 | 215 ± 30 | 225 | 1,450 | 1,450 | 80 | 0.6 | ND | |
| | 250-350 | 250 | 300 | 250 | 300 | 250 | 300 | 250 | 300 | 250 | 300 | 215 ± 30 | 225 | 300 | 8,000-15,000 | 8,000-15,000 | 80 | 0.6 | ND | |
| | 250 | 225 | 300 | 250-350 | 250 | 300 | 250 | 300 | 250 | 300 | 250 | 300 | 215 ± 30 | 225 | 1,450 | 1,450 | 80 | 0.6 | ND | |
| | 5.5 ± 0.5 | 35,400 | 390 ^a | 170 ^a | 130,000 ^b | 3,610 ^c | 800 ^a | 19,960 ^a | 2,900 ^a | 9,700 ^a | 33 ^a | 190 ^a | 60 ^a | 302 ^a | 6.4 | 12,000-25,000 | 4.9 | 6.4 | 6,000-30,000 | |
| | 32,000-66,000 | 3,540 | 35 ^{b,p} | 1.8 · 10 ^{-7p} | 4,000 ^a | 0 ^a | 800 ^b | 2,020 ^b | 80 ^b | 15 ^a | 0.00045 ^a | 0.00047 ^a | 3.3 · 10 ^{-5a} | 0.7 ^a | 11,700 | 12,000-25,000 | 35,400 | 1,080 | 32,000-66,000 | |
| | 5-250 | 390 ^a | 170 ^a | 130,000 ^b | 3,610 ^c | 800 ^a | 19,960 ^a | 2,900 ^a | 9,700 ^a | 33 ^a | 190 ^a | 60 ^a | 302 ^a | 300 | 1,620 | 1,080 | 3,200 | 190 | 5-250 | |
| | 950-1,900 | 4,000 ^a | 0 ^a | 800 ^b | 2,020 ^b | 80 ^b | 15 ^a | 0.00045 ^a | 0.00047 ^a | 3.3 · 10 ^{-5a} | 0.7 ^a | 11,700 | 12,000-25,000 | 35,400 | ND | ND | 1.6 · 10 ⁻⁵ | 10 | 950-1,900 | |
| | 100,000-300,000 | 800 ^b | 1.8 · 10 ^{-7p} | 4,000 ^a | 3,610 ^c | 800 ^a | 19,960 ^a | 2,900 ^a | 9,700 ^a | 33 ^a | 190 ^a | 60 ^a | 302 ^a | 300 | 100,000-300,000 | 100,000-300,000 | 88,000 | 10,800 | 100,000-300,000 | |
| | ND | 800 ^b | 1.8 · 10 ^{-7p} | 4,000 ^a | 3,610 ^c | 800 ^a | 19,960 ^a | 2,900 ^a | 9,700 ^a | 33 ^a | 190 ^a | 60 ^a | 302 ^a | 300 | 100,000-300,000 | 100,000-300,000 | 88,000 | 10,800 | 100,000-300,000 | |
| | ND | 800 ^b | 1.8 · 10 ^{-7p} | 4,000 ^a | 3,610 ^c | 800 ^a | 19,960 ^a | 2,900 ^a | 9,700 ^a | 33 ^a | 190 ^a | 60 ^a | 302 ^a | 300 | 100,000-300,000 | 100,000-300,000 | 88,000 | 10,800 | 100,000-300,000 | |
| | 19,000-38,500 | 33 ^a | 190 ^a | 60 ^a | 302 ^a | 300 | 215 ± 30 | 225 | 300 | 250-350 | 250 | 300 | 215 ± 30 | 225 | 8,000-15,000 | 8,000-15,000 | 240 | 500 | 4,000-20,000 | |
| | 3,500-7,300 | 190 ^a | 60 ^a | 302 ^a | 300 | 215 ± 30 | 225 | 300 | 250-350 | 250 | 300 | 215 ± 30 | 225 | 300 | 8,000-15,000 | 8,000-15,000 | 23,000 | 640 | 19,000-38,500 | |
| | ND | 60 ^a | 302 ^a | 300 | 215 ± 30 | 225 | 300 | 250-350 | 250 | 300 | 250 | 300 | 215 ± 30 | 225 | 1,450 | 1,450 | 670 | 145 | 3,500-7,300 | |
| | ND | 302 ^a | 300 | 215 ± 30 | 225 | 300 | 250-350 | 250 | 300 | 250 | 300 | 215 ± 30 | 225 | 300 | 8,000-15,000 | 8,000-15,000 | 670 | 0.6 | ND | |
| | 90-8,900 | 33 ^a | 190 ^a | 60 ^a | 302 ^a | 300 | 215 ± 30 | 225 | 300 | 250-350 | 250 | 300 | 215 ± 30 | 225 | 1,450 | 1,450 | 80 | 0.6 | ND | |
| | 1.6-0.3 | 190 ^a | 60 ^a | 302 ^a | 300 | 215 ± 30 | 225 | 300 | 250-350 | 250 | 300 | 215 ± 30 | 225 | 300 | 8,000-15,000 | 8,000-15,000 | 670 | 0.6 | ND | |
| | 0.5-0.05 | 60 ^a | 302 ^a | 300 | 215 ± 30 | 225 | 300 | 250-350 | 250 | 300 | 250 | 300 | 215 ± 30 | 225 | 1,450 | 1,450 | 80 | 0.6 | ND | |
| | ND | 302 ^a | 300 | 215 ± 30 | 225 | 300 | 250-350 | 250 | 300 | 250 | 300 | 215 ± 30 | 225 | 300 | 8,000-15,000 | 8,000-15,000 | 670 | 0.6 | ND | |
| | ND | 302 ^a | 300 | 215 ± 30 | 225 | 300 | 250-350 | 250 | 300 | 250 | 300 | 215 ± 30 | 225 | 300 | 8,000-15,000 | 8,000-15,000 | 670 | 0.6 | ND | |

Abbreviations: a = arkose, g = graywacke, p = pelite; ND = not determined
^a Arkose assemblage at pyrrhotite-pyrite- $X_{Fe}^{bio} = 0.37$, $f_{CO_2} = 10$ b, 0.33m Cl
^b Pelite assemblage at graphite-pyrrhotite-pyrite- $X_{Fe}^{bio} = 0.43$, $f_{CO_2} = 100$ b, 0.33m Cl
^c Main gold stage, estimated from fluid inclusion data, Kuehn and Rose, 1995
^d Estimated from fluid inclusion data and mineral stability, Hofstra et al., 1991
^e Spycher and Reed, 1989; Brown, 1986
^f Nesbitt & Muehlenbachs, 1989
^g Barton et al., 1977

in $\Sigma\text{Au}_{\text{aqueous}}$ with increasing f_{O_2} (Fig. 7B). This is opposite what would be predicted from simple stoichiometry of the gold dissolution if changes in ΣS are not considered.

Although arkose-sourced fluids contain much higher gold concentrations, it appears that all source lithologies investigated can generate ore-forming fluids, provided that the source is sufficiently reduced. Fluids containing as little as 3 ppb Au could produce 1 ppm grades based on estimated water to rock mass ratios in the deposits of $\sim 300:1$ (Ilchik, 1990b) if all gold is deposited at the deposit level (cf. Fig. 7).

Many of the systematics of Au solubility in our calculated source fluid are displayed in Figure 6. The similarity in slope for contours of aqueous H_2S and $\text{Au}(\text{HS})_2^-$ activity illustrate the importance of $\Sigma\text{S}_{\text{reduced}}$ on gold solubility. Because the reaction curve between magnetite and pyrite is nearly parallel to these contours, fluids equilibrated with magnetite-bearing rocks have low concentrations of $\Sigma\text{S}_{\text{reduced}}$ and gold bisulfide complexes. In contrast, fluids equilibrated with rocks containing pyrite and pyrrhotite with f_{O_2} buffered by an iron phyllosilicate or graphite at a low to moderate f_{CO_2} will have a substantially higher $\Sigma\text{S}_{\text{reduced}}$, and thus higher gold contents. The ΣS and Au will increase as the Fe content of the phyllosilicate and/or f_{CO_2} decreases.

Base metals: Aqueous base metal concentrations varied from <1 to 250 ppm and correlated inversely with Au concentrations (Fig. 7C). Factors that enhanced lead and zinc concentrations (low $\Sigma\text{S}_{\text{reduced}}$ and high ΣCl) tended to suppress aqueous gold. Base metals were highest in high-chlorinity fluids which had equilibrated with magnetite-bearing pelites and lowest in low-chlorinity fluids from arkosic assemblages with low Fe annite. Only those fluids with a greater than 0.3 mole ΣCl which had equilibrated with pelite or those with a 1.0-mole ΣCl which had equilibrated with graywacke would be ore fluids if a 10 ppm minimum concentration of base metals is required. On the other hand, the highest concentration of base metals in an arkose-equilibrated fluid (1.0 mole ΣCl , at magnetite-pyrite-hematite) is just over 1 ppm. These calculations show that when gold is transported as a bisulfide complex, accompanying base metal mineralization is unlikely.

Other components: Nonore components of the source fluids also vary significantly with chlorinity and relative acidity of the source assemblage. The sole exception to this was aqueous silica, which was always buffered by quartz. Total chloride was the dominant control on total cation concentrations. The mineralogical controls on pH resulted in arkose-equilibrated fluids having the highest concentrations of Na and K, whereas pelite-equilibrated fluids were highest in Ca, Mg, and Fe (a consequence of 1:1 vs. 1:2 cation to hydrogen ion stoichiometries). Likewise, the mole fraction of CO_2 in the fluids varied from 0.001 to 0.036, increasing from the near-neutral arkosic assemblages to the highest values for the pelitic assemblages; it also increased with increasing f_{O_2} for graphitic assemblages. The ΣCl , through its effects on pH, had only marginal influence on the concentration of aqueous carbonate. The ΣS increased only slightly with a decreasing ΣCl , reflecting buffering by Fe sulfides.

These calculations demonstrate that interaction between low-chlorinity fluids and moderately reduced, sulfide-bearing

source rocks can produce aqueous gold concentrations sufficient to form Carlin-type mineralization under conditions compatible with Great Basin extension. The compositions of these fluids are unexceptional; they simply follow from the lithologies present in the north-central Great Basin. In more oxidized or saline fluids, base metals would be mobilized, but unless these fluids are exceptionally saline and oxidized, gold would not be present in significant concentrations (see below).

Comparison with independent estimates of ore fluids: Compositions of some of the calculated fluids compare well with fluid compositions determined for Carlin-type deposits, as well as with some fluids associated with mesothermal gold quartz veins and some modern geothermal fluids (Table 4). The key similarities with fluid compositions determined or inferred for the Jerritt Canyon (Hofstra et al., 1991) and Carlin (Kuehn and Rose, 1995) deposits include pH, oxidation state (near pyrrhotite-pyrite), ΣCO_2 (for graywacke and pelitic sources), ΣCl , silica concentrations, and base metal contents (for arkosic sources). The biggest differences are lower contents of ΣCO_2 (for arkosic sources), ΣS , and, as a consequence, lower gold concentrations. The elevated CO_2 and moderate ΣCl contents also resemble fluids from mesothermal gold quartz veins. They are, however, distinct from the fluids associated with Creede-type base and precious metal systems, which have a higher salinity.

Reduced, arkose-equilibrated, low chloride fluids appear to be the most attractive sources because of their high gold, high sulfur, and low base metal contents, but they have CO_2 contents which are lower than those determined for Carlin-type deposits (although limited calculations at 350°C and 1.5 kbars indicate that these moderate increases in temperature and pressure promoted marked increases in ΣCO_2). Pelite- and graywacke-equilibrated fluids from reduced sources have CO_2 contents which resemble those determined for Carlin-type systems; given an efficient precipitation mechanism, they could also act as ore fluids. Thus a variety of lithologies, all under geologically reasonable conditions, could generate potential ore-forming fluids.

Deposit-Level Calculations

Approach

Simulations of fluid-rock interactions in the deposit environment were conducted at 500 bars and at various temperatures between 150° and 225°C . The processes evaluated included: (1) simple cooling, (2) cooling with various wall-rock reactions, and (3) mixing with a second, dilute fluid. Simple cooling was simulated by re-equilibrating source fluid compositions at deposit conditions. Cooling with wall-rock interaction was simulated by equilibrating source fluids at deposit temperatures with mineral assemblages appropriate to the common host rocks of Carlin-type deposits. Mixing with a second, pure H_2O fluid was simulated by diluting the masses calculated for the high-temperature fluids while accounting for the increased total fluid mass. We found, not surprisingly, that a number of mechanisms and host rocks can precipitate ore-grade gold, but that only a limited number of scenarios are consistent with the typical characteristics of Carlin-type systems.

Because the number of phases in the deposit-level simulations was smaller than the number of components in the fluids, the number of mass balance equations in the deposit-level calculations was increased to conserve aqueous components which are not buffered by phases in the host rock (e.g., Na and in many cases Ca, Mg and K). Changes in f_{O_2} , pH, and ΣS have major effects on gold solubility; therefore, the controls on these parameters are discussed in some detail.

Three alternative controls on oxidation state of the deposit-level fluid were investigated. The only method which proved generally acceptable based on comparison with real deposits was the assumption of homogeneous equilibrium among dissolved carbon and sulfur species plus reaction with pyrite and base metal sulfides. Results from this method of controlling f_{O_2} and ΣS are reported below. Two other methods for controlling f_{O_2} —homogeneous equilibrium among dissolved carbon and sulfur species plus reaction with sulfides and graphite, and homogeneous equilibrium among dissolved sulfur species, but not carbon species—produced results grossly inconsistent with observation. In the first case, inclusion of graphite (as a proxy for organic matter) in the calculations resulted in the precipitation of unrealistically large amounts of graphite (i.e., greater than quartz). In addition, because CO_2 exceeds CH_4 in the fluid, inclusion of graphite led to large increases in f_{O_2} , which in turn dramatically increased gold solubility. In the case where only aqueous sulfur species and sulfide minerals were allowed to equilibrate, f_{O_2} remained close to that of the source assemblage (e.g., pyrite-pyrrhotite) and gold precipitated regardless of all other conditions such as host-rock alteration. This is inconsistent with the observed correlation between gold mineralization and decalcification. Other species (most notably H_2 or N_2), which could play a role in the control of oxidation state at the deposit level, were not included in these calculations due to limitations in our modeling techniques.

Deposit-level results

Simple cooling: In the simple cooling simulations, the higher temperature fluids were reequilibrated at temperatures between 225° and 150°C and 0.5 kbars. Quartz, pyrite, galena, and sphalerite supersaturated at all temperatures, and hence were allowed to precipitate. Gold was at or near saturation in about half of the solutions at 225°C, but became increasingly soluble as temperature decreased (Fig. 8). Decreasing pressure initially lowers gold solubilities, but isobaric cooling increases them. Low chloride, arkose- and graywacke-equilibrated fluids along with a few high chloride pelite-sourced fluids were the most likely to supersaturate with gold. For low chloride fluids, saturation appears to be due to changes in pH resulting from increased dissociation of H^+ -bearing aqueous complexes (Fig. 9A). For a few high chloride fluids, gold saturation was the result of sulfur removal due to high initial contents of base metals and iron which precipitated as sulfide (Fig. 9B). In all cases where desulfidation of the ore fluid led to gold saturation, less than 1 μg of gold per kg of fluid was deposited because of low initial gold contents of these fluids. Thus, only at very high water/rock (~1,000:1) would these fluids produce economic mineralization.

Base metals in the simple cooling models behaved antithetically to gold (Fig. 9C). A strong temperature dependence

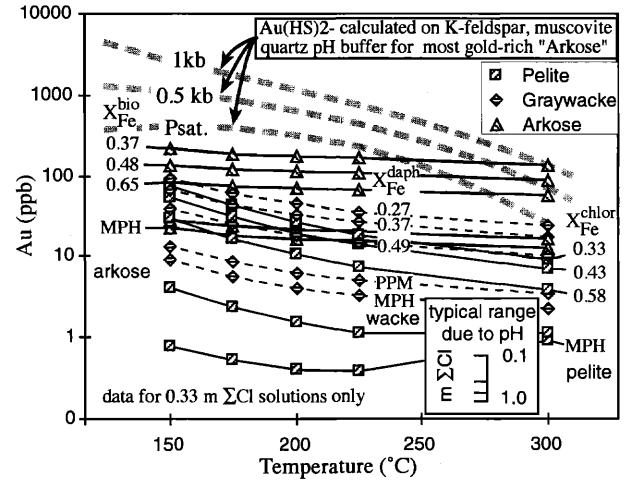


Fig. 8. Effects of cooling and decreased pressure on gold solubility for various lithologies and f_{O_2} , f_{S_2} buffers; for simplicity only the 0.33 m ΣCl solutions are shown (annotations as in Fig. 7.) All solutions were initially calculated at 300°C and 1 kbar; fluids compositions were conserved and homogeneous equilibrium maintained between 225° and 150°C with pressure fixed at 0.5 kbars. The initial drop in gold solubility from 300° to 225°C is largely due to pressure. Further isobaric cooling below 225°C, however, often led to increased gold solubility. Heavy dashed curves depict the temperature evolution of gold solubility at various pressures assuming pH is controlled by muscovite + quartz = K feldspar and the K concentration of the most gold-rich solution (1 kbar data from Seward, 1973; H_2O liquid-vapor equilibrium, Psat. from Shenberger and Barnes, 1989; 0.5 kbars interpolated).

was found for the base metal sulfides, such that greater than 85 percent of the base metals generally precipitated by cooling to 200°C. Only the high chloride, oxidized pelite-derived fluids did not precipitate the full complement of base metals due to iron exceeding the amount of sulfur needed to precipitate galena and sphalerite. As at the source level, the contrasting solution chemistry of gold and base metals at these lower temperatures predicts that gold-rich deposits should be base metal poor and distinct from base metal-rich deposits which should be gold poor. The only nonmetallic component of the fluids to reach saturation during simple cooling was silica. Quartz solubilities decreased from about 0.8 g/kg at 300°C to less than 0.3 g/kg at 200°C. Thus, simple cooling led to precipitation of substantial amounts of quartz, which in many cases would be accompanied by modest amounts of gold.

Cooling with wall-rock reaction: Cooling with wall-rock reaction was simulated by reequilibrating the fluids at 200°C with host-rock mineral assemblages commonly present in Carlin-type deposits. Simulated lithologies included limestone (calcite + quartz), jasperoid (quartz), unaltered dolomitic siltstone (quartz + muscovite + dolomite), and altered noncalcareous siltstone (quartz + muscovite + kaolinite). These mineral associations are typical, although some possible assemblages (e.g., kaolinite-muscovite-carbonate) define equilibria well outside the range defined by source fluids. As shown below, this contributes to gold precipitation. When saturated, the phases pyrite, galena, and sphalerite were also allowed to precipitate.

Interaction between the calculated fluids and limestone

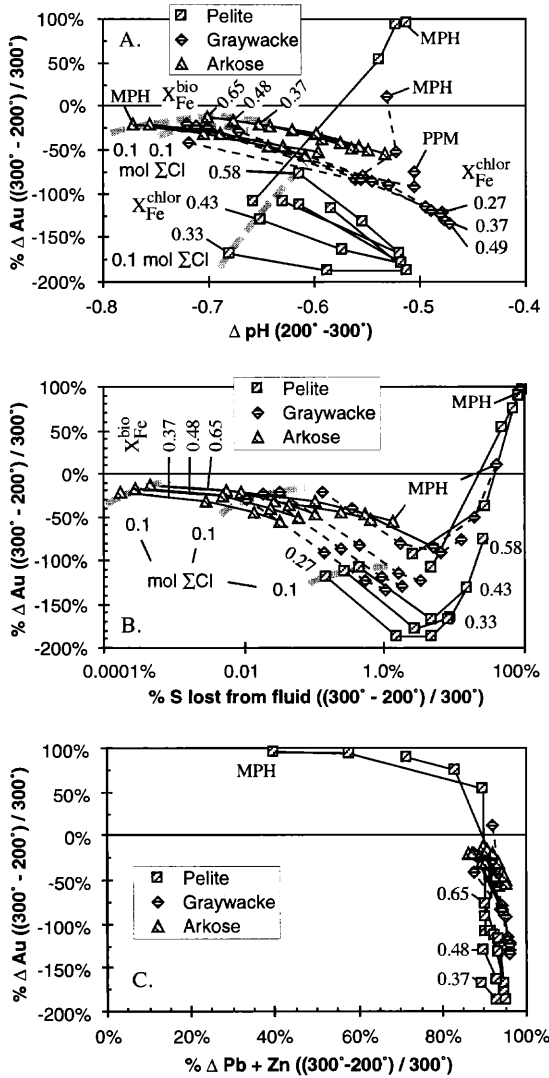


FIG. 9. Simple cooling of source fluids to 200°C and 500 bars (annotations as in Fig. 7). This case is also equivalent to reaction with jasperoid. A. Percent change in gold solubility ((300°–200°C)/300°C) vs. change in pH (300°–200°C). Only solutions with high iron + base metal contents became saturated with respect to gold, but most arkose-derived fluids were near saturation. Lower initial ΣCl tended to produce greater decreases in pH and brought solutions closer to gold saturation. B. Percent change in gold solubility vs. percent change in ΣS showing that large losses in sulfur led to the gold deposition. C. Percent change in gold vs. percent change in base metals. Except for those fluids with high initial base metal and iron contents, deposit conditions tend to separate gold farther from base metals. Similar relationships between the deposition of base metals and gold were seen in all cases modeled regardless of wall-rock conditions.

was simulated by adding calcite to the minerals that precipitated in the simple cooling model (i.e., quartz, pyrite, galena, sphalerite). Gold supersaturation occurs only when the amount of dissolved iron and base metals is sufficient to remove most aqueous sulfur (Fig. 10A). As in the simple cooling simulations, this form of desulfidation caused gold precipitation only in high-chlorinity fluids from certain pelites and graywackes. In most cases, buffering by calcite resulted in modest changes in pH from source to deposit which led to increased gold solubility (Fig. 10B). Predicted wall-rock

alteration is calcite leaching and quartz deposition (Fig. 10C). The predicted alteration product is gold-poor quartz replacing limestone, analogous to the replacement and fault-related jasperoids commonly present in Carlin-type deposits.

Interaction between the calculated fluids and a dolomitic host (siltstone or marl) was simulated by including dolomite

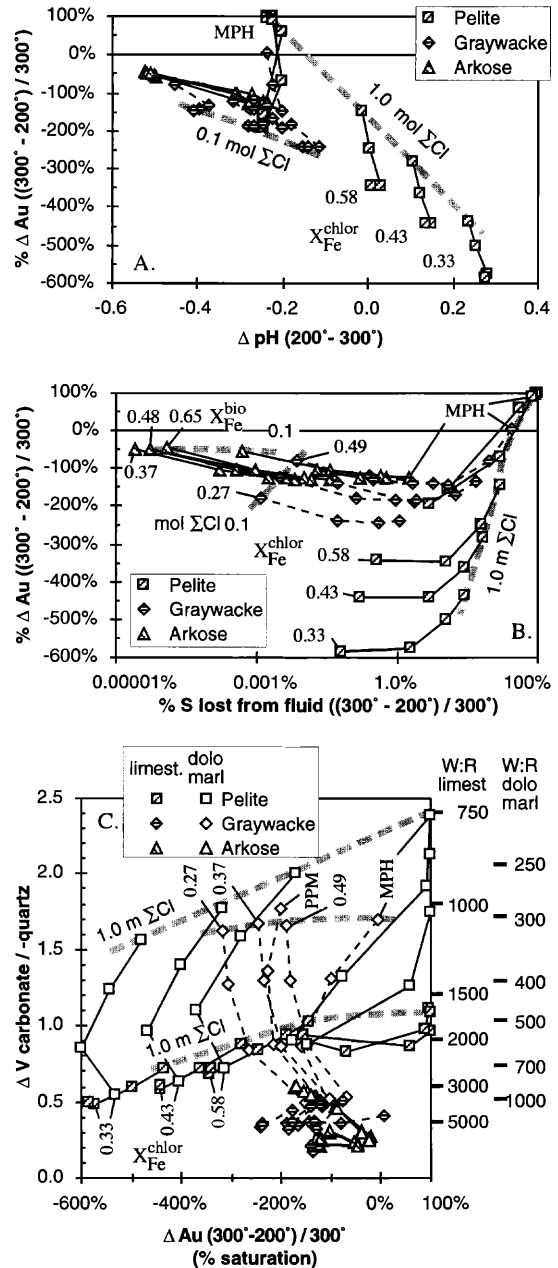


FIG. 10. Simulations of reaction between source fluids and massive limestone (e.g., initiation of jasperoid formation) at 200°C and 0.5 kbars (annotations as in Fig. 7). A. Percent change in gold solubility as a function of the change in pH. Comparison with Figures 9A and 11A indicates that calcite tends to buffer pH to values which inhibit the deposition of gold in nearly all cases. B. Percent change in gold solubility as a function of the percent change in ΣS showing again that only large losses of sulfur led to the deposition of gold. C. Volume changes caused by leaching of carbonate and deposition of quartz for source fluid reactions with a limestone (filled symbols) and a dolomitic marl (open symbols).

and muscovite with the phases that saturate by simple cooling. The results of these simulations were similar to those in the limestone case. Acidity varied slightly from the limestone case as a function of chlorinity and source rock (Fig. 10C). Once again, gold became saturated only in fluids that originally contained iron and base metals in excess of ΣS . The most important difference in interactions involving dolomitic rocks is that the amount of carbonate leached is two to three times greater than in cases involving calcite (Fig. 10C). As a consequence, reactions involving dolomitic rocks would tend to promote the development of secondary permeability since the volume of quartz deposited was often significantly less than the volume of dolomite leached. For marly host rocks, this predicts that fluids should have continued access to dedolomitized host rocks after the pH buffer is removed. The limited deposition of gold in either type of carbonate-bearing host rock, limestone and dolomitic marl, is consistent with general field observations that gold is present only sparingly in such rocks.

Typical host rocks for gold mineralization are calcareous sediments in which the carbonate has been completely removed during alteration. For siliceous rocks which lack sheet silicates this is equivalent to the simple cooling models described above; thus the simple cooling models also simulate fluid interaction with a nearly pure quartz jasperoid. For cases involving decarbonated marls or siltstones, assemblages of quartz, muscovite, and kaolinite and the saturated sulfide phases (base metal sulfides were undersaturated in the arkose-derived fluids and were not included for those runs) were reacted with the source fluids. In these cases, the final pH of the fluid was controlled by reaction between muscovite and kaolinite as mediated by the activity of K^+ . For arkose-derived fluids this led to a decrease of 0.8 to 1.2 pH units below that of the simple cooling-jasperoid model. This precipitated 20 to 70 percent of the gold in solution. For graywacke- and pelite-derived fluids, the lower activity of K^+ resulted in an increase in pH of 0.05 to 0.2 pH units and 0.3 to 0.7 pH, respectively. This contributes to increased gold solubility by 50 to 150 and 150 to 400 percent, respectively, over that of the source fluids. As before, the only exception was for metal-excess fluids. All scenarios precipitated quartz and drove reactions between muscovite and kaolinite. Arkose-derived fluid contained enough potassium to convert kaolinite to muscovite, whereas pelite- and graywacke-sourced fluids, with lower K^+ contents, converted muscovite to kaolinite.

In most simulations with limestone, a smaller volume of calcite was dissolved than the volume of quartz precipitated. This implies that permeability would tend to be occluded and gold contents would be moderate to low in massive limestones where cooling or simple wall-rock reaction dominates. Permeability would be enhanced when calcite dissolution exceeds silica precipitation; thus, for example, fluid mixing would help focus fluid flow as well as promote gold precipitation (see below).

Field observations show that gold commonly closely follows decalcification in host rocks, broadly consistent with the model results. The ability of source fluids to leach carbonate minerals from unaltered host rocks and form environments which are apparently more receptive to gold deposition appears to be an important characteristic of both Carlin-type

ore fluids and our calculated fluids. Many source-rock-derived fluids should precipitate gold in decalcified environments as long as permeability allows fluids to infiltrate these altered rocks. Fluids which transit through these chemically prepared host rocks and enter marginal calcareous environments would again have their pH buffered to higher values due to reactions with carbonate minerals. This would lead to increased gold solubility, cessation of gold precipitation, and production of the alteration controls on ore distribution found in most deposits.

Sulfidation of wall rocks: Desulfidation of source fluids by reaction with wall-rock iron has been proposed to contribute to gold deposition in Carlin-type deposits (Hofstra et al., 1991). Several cases where the reactive components (iron and base metals) are cotransported in the fluid are shown in Figures 9B, 10B, and 11. In these cases, 10 to 40 percent of the aqueous sulfur has to be removed before the fluids reach gold saturation. For the more common case where the amount of aqueous sulfur greatly exceeds that of iron, the reactive components must be provided by the host rocks. If sufficient iron is available to precipitate half of the gold in solution at 300°C, then, for the arkose-derived fluid, 1 to 5 g of iron per kg of rock is required for each milligram of gold precipitated (larger amounts of Fe are required by high ΣCl fluids, but are unaffected by f_{O_2} buffers). The amount of iron per mg of gold increases to between 5 and 20 g for the graywacke-equilibrated fluids and to between 20 and 45 g for pelitic fluids. Desulfidation is most effective for solutions which have higher initial contents of gold and which are already near saturation. For these cases, less than 1 wt percent epigenetic pyrite may be codeposited with gold. For solutions with lesser amounts of gold, 5 to 10 wt percent epigenetic pyrite may be attendant with gold mineralization.

Mixing with ground water: The effects of mixing between calculated source fluids and a dilute ground water (i.e., containing no solutes) were simulated by progressively reducing the concentrations of all solutes in the source fluid before recalculating chemical equilibria. These diluted fluids were then reacted either by simple cooling or by reactions with dolomitic marl to determine postmixing concentrations in the

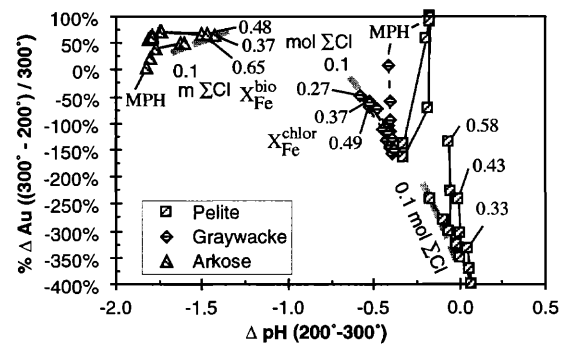


FIG. 11. Percent change in gold solubility vs. change in pH for reaction of source fluids with dedolomitized marl at 200°C and 500 bars (annotations as in Fig. 7). The larger drop in pH for arkose-derived fluids was due to their higher K^+ contents and effectively led to precipitation of gold. For the pelite- and graywacke-derived fluids, K^+ is lower and the change in pH was not sufficient to precipitate gold.

fluids. All mixing calculations were carried out at 200°C and 500 bars.

Mixing combined with simple cooling can efficiently remove gold from all source fluids (Fig. 12A). The mass fraction of dilute fluid needed to precipitate gold varies from about 0.4:1 of the ore fluid mass for the nearly saturated arkose-derived fluids to over 2:1 for the strongly undersaturated pelite-derived fluids. Gold precipitates in response to dilution of aqueous sulfur, although this is partly offset in some assemblages by increases in pH and f_{O_2} .

Fluid mixing within the dolomitic marl led to gold deposition only after large amounts of dilution, but mixing increased the rate of carbonate leaching. Mass ratios of ~2.3:1 (i.e., $X_{\text{ore fluid}} \approx 0.30$) were required to cause the arkosic fluids to saturate with gold, whereas 4:1 or greater was required for graywacke- and pelite-sourced fluids (Fig. 12B). Mixing did aid chemical preparation of the rock by increasing the amount of carbonate minerals removed while decreasing the amount of quartz deposited. At 1:1 mixing, all fluids produced secondary permeability since the volume of dolomite removed exceeded that of quartz deposited; at about 2:1 mixing, the resulting fluids became undersaturated with respect to quartz.

Mixing combined with wall-rock reactions thus promotes carbonate loss, suppresses silica precipitation, and can effectively precipitate gold in noncalcareous rocks. This mechanism, or the somewhat less efficient wall-rock reaction without fluid mixing, can produce the observed patterns of alteration and gold distribution. These results predict the common

pattern of decalcified gold-rich zones surrounded by carbonate-bearing, gold-poor zones. Finally, mixing alone could account for mineralization being localized in other zones of preexisting high permeability, such as highly fractured contact aureoles or faults (e.g., Gold Strike).

Implications for fluid flux, grade, and deposit genesis

Simulations of depositional mechanisms indicate that many fluids which equilibrated with reduced source rocks can generate both the metal contents and wall-rock alteration observed in Carlin-type systems. Simple cooling can precipitate gold; however, combinations of cooling with wall-rock reaction in noncalcareous lithologies, sulfidation, or mixing with a dilute fluid are more efficient at depositing gold. Alteration, particularly in calcite-bearing hosts, does distinguish to some degree among most sedimentary (or indeed most igneous) lithologies as fluid sources. Qualitative consideration of factors, such as disequilibrium at the deposit level or deposition of some quartz along flow paths, suggests that these processes would enhance rather than diminish the fit to observed characteristics. Many sources can produce fluids that remove carbonate and precipitate quartz at the deposit level provided that some aqueous CO_2 or other acid-generating species is present. Gold mobility, however, is sensitive to source redox state (as controlled here by iron content in phyllosilicates), chlorinity, and pH.

Fluid fluxes: From the calculated carbonate solubilities, fluid to rock mass ratios (W/R) range from ~1,500:1 to 5,000:1 to replace calcite and ~750:1 to 3,000:1 to replace dolomite. Decalcification of an impure carbonate (i.e., marls) would require proportionally smaller amounts of fluid (Fig. 10C). W/R estimates using aqueous silica are ~1,000:1 and ~300:1, respectively, assuming deposition of 0.5 g of quartz per kg of fluid, a 50 percent volume reduction relative to the replaced carbonate component, and nodeposition of quartz along flow paths. For the 300°C source conditions, the latter assumption is reasonable when fluid ascent is rapid ($>10^{-4}$ m/s, Rimstidt and Barnes, 1980). Higher temperatures or pressures at the source would increase the amount of silica transported and decrease the W/R, but an increase to 350°C and 1.5 kbars only decreases the W/R by about half. At still higher temperatures, the amount of silica transported to the deposit and hence estimates for W/R should not change significantly because quartz precipitation rates increase rapidly above 350°C and quartz should be readily deposited along any higher temperature portions of the flow path (Rimstidt and Barnes, 1980). The likelihood of incomplete precipitation of silica at the deposit site and partial deposition along the flow path suggests that the values given above based on silicification are minimums for W/R.

W/R ratios for the gold deposition stage of mineralization based on the formation of 1 ppm mineralization in an altered marl host vary from ~10 to 1,000 for arkose-derived fluids. For other cases where gold was saturated at the deposit level, W/R estimates vary from 1,000 to ~8,000. This is largely due to the original low gold contents of the pelite- and graywacke-derived fluids. For the jasperoid-simple cooling model, many fluids were near saturation at 200°C, but too few actually would deposit gold to make a meaningful estimate of W/R.

Whatever the exact processes which took place at the de-

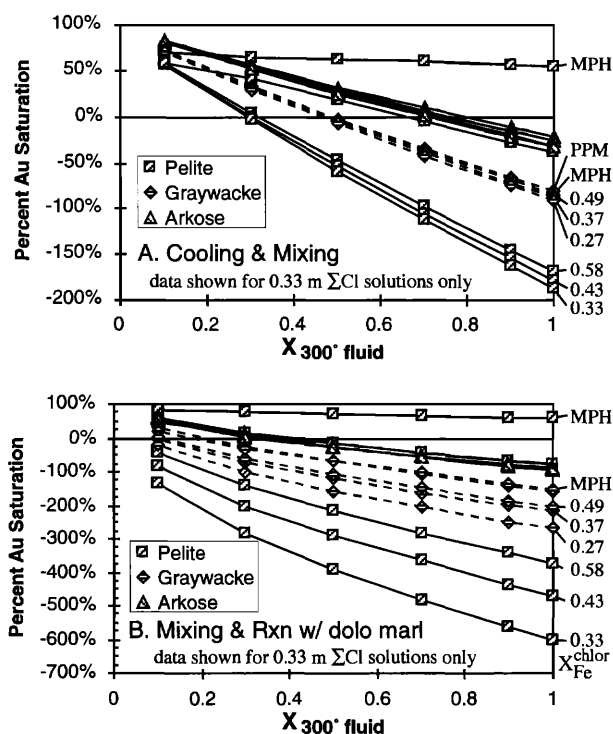


FIG. 12. Simulation of mixing of source fluids with a dilute water at 200°C and 500 bars (annotations as in Fig. 7). A. Reaction of mixed fluid under simple cooling-jasperoid conditions. B. Reaction of mixed fluid with dedolomitized marl (quartz + muscovite + kaolinite + pyrite \pm base metal sulfides).

posit, these model results and the geologic and geochemical patterns require high W/R at the deposit. These high W/R appear to be achieved by channeling of fluids along faults, in brittle or intrinsically porous rocks (perhaps explaining localization in some contact metamorphosed rocks), and by enhancement of porosity by loss of carbonate. The latter mechanism may be important because it would be self-reinforcing where the volume of carbonate lost exceeds that of new quartz.

In contrast, the W/R must be low and flow must be diffuse in the source areas. Calculated aqueous gold concentrations for potential ore-forming fluids typically exceed reasonable concentrations in sources, indicating that the effective W/R must be <1 . For an orebody with an average gold grade of 1 ppm, the mass of the source is 1,000 times the deposit mass if transport and deposition are completely efficient and the source contained 1 ppb gold. This is consistent with the sediment-dominated oxygen isotope signature of the ore fluids (Holland et al., 1988; Ilchik, 1990a; Hofstra, 1994; Kuehn and Rose, 1995). Mineralogy and bulk composition of the source rocks, however, should be little changed by this interaction, because of the relatively low concentrations of major elements (and sulfur) in the fluids. Consequently, changes in fluid chemistry at the deposit level are more likely to indicate variations in process (e.g., amount of mixing) or an evolving mix of sources rather than mineralogical changes in any given source.

Metallogenic Implications

Differences in geochemistry, geologic setting, and to a lesser degree, depositional mechanisms lead to many types of epigenetic gold deposits (Keays et al., 1989). These factors rationalize the spatial and temporal distribution of amagmatic (Carlin- and detachment-type) systems in southwestern North America (Fig. 1).

Magmatic and metamorphic connections revisited

The contrast between the stability of AuCl_2^- and $\text{Au}(\text{HS})_2^-$ helps to distinguish typical igneous-related systems from Carlin-type systems (Fig. 13). Chloride complexes play a dominant role in metal transport in moderately oxidized magmatic hydrothermal systems which form many porphyry, skarn, and advanced argillic epithermal deposits. For these systems, high ΣCl concentrations and a high oxidation state promote metal solubility; temperature is an important factor in metal deposition. In contrast, conditions favoring $\text{Au}(\text{HS})_2^-$ are low ΣCl (neutral pH), moderate to low oxidation states (high $\Sigma S_{\text{reduced}}$), and lower temperatures. The solution chemistry of these gold complexes predicts a solubility minimum at about 350°C . This minimum impedes transport of gold from high to low temperature. A reduced magmatic source for fluids, such as those that produce some high-temperature igneous-related deposits (cf. Matthäi et al., 1995), might aid the transition to lower temperatures, but gold mineralization has yet to be documented with reduced (ilmenite series), peraluminous, or metaluminous granitoids in the Great Basin (Barton, 1990; M. Barton and G. Ghidotti, unpub. data, 1996).

Mid-Tertiary magmatism and extension are closely linked

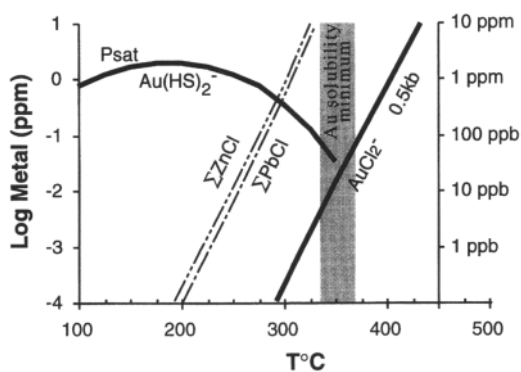


FIG. 13. Solubility of gold as $\text{Au}(\text{HS})_2^-$, AuCl_2^- and base metal as a function of temperature. The zonation of a gold-rich interior and a base metal periphery in many porphyry-related environments (Sillitoe, 1988) is consistent with the temperature dependence of the chloride complexes. The concentration minimum between the two gold complexes appears to inhibit evolution of magmatic fluids into fluids documented for Carlin-type deposits. The lack of base metal enrichments in or around Carlin-type deposits suggests that high-temperature, chloride-rich fluids were not important in these systems. Conditions for chloride complexes: $a_{\text{Cl}^-} = 1$ m, $a_{\text{H}^+} = 0.1$ m, $a_{\text{HS}^-} = 0.1$ m, $f_{\text{O}_2} = \text{hematite} + \text{magnetite}$, and $P = 500$ bars; for $\text{Au}(\text{HS})_2^-$: $\Sigma S_{\text{reduced}} = 0.01$ m, $a_{\text{Cl}^-} = 0.1$ m, $a_{\text{H}^+} = 0.01$ m, $f_{\text{O}_2} = \text{SO}_4^{2-} - \text{H}_2\text{S}$ equal activity; for both: pH at K feldspar-muscovite-quartz. Data sources: Zotov et al. (1991), Shenberger and Barnes (1989), Seward (1973), and Johnson et al. (1992).

in time and space in the Great Basin (Seedorff, 1991), and a magmatic heat contribution could well help localize and intensify the hydrothermal systems that formed some Carlin-type deposits. Igneous heat is both unnecessary given ample heat loss from the upper crust (Fig. 3) and not indicated given the distributed rather than focused loci of deposits which lack correlation with Tertiary igneous centers. Nonetheless, local association of mid-Tertiary igneous rocks with some Carlin-type deposits or other systems with geochemical affinities would not be surprising: igneous-driven circulation of meteoric waters through the reduced sedimentary rocks could produce analogous deposits. Genetic links to Mesozoic plutons are also possible based on geochronometry and lithologic associations (Arehart et al., 1993a; Wilson and Parry, 1995), but it appears more likely that the occasional spatial association is due to enhanced permeability or appropriate reactive compositions (e.g., iron-rich skarns) related to earlier geologic events. However, local areas of extension occurred in the northern Great Basin during the Middle to Late Jurassic (Saleeby et al., 1992); if dilute waters had been available, similar deposits might have been produced at that time.

Seedorff (1991) and Phillips and Powell (1993) have advocated metamorphic fluid sources for Carlin-type systems by analogy with some metamorphic gold quartz deposits. Indeed, greenschist facies fluids generated from a reduced, sulfur-bearing, feldspar-stable source would have compositions resembling those of the fluids calculated here. The strongest arguments against a purely metamorphic fluid origin are the marginal adequacy of the source even at 5 wt percent fluid (Fig. 3), and the isotopic evidence indicating predominantly meteoric waters. In addition, geochronometry indicates regional cooling during mid-Tertiary extension and the lack of a well-defined heat source able to cause adequate metamorphism (Miller et al., 1987; Dokka and Baksi, 1988).

Implications of the amagmatic model

An amagmatic origin has a number of implications for Carlin-type deposits and for other aspects of the Phanerozoic metallogeny of southwestern North America.

Gold resource potential. Energy balance considerations are compatible with a considerably larger gold resource than has been discovered in the northern Great Basin (Fig. 3). The thermal energy available to heat waters at 100 percent extension is $\sim 10^{24}$ joules for the roughly 160,000-km² productive area. This could generate ~ 100 km³ ($\sim 3 \times 10^{11}$ tons) of jasperoid-type alteration (assuming quartz-bearing sources). If the average gold grade of this silicification is 100 ppb (plausible from the models and observation), then roughly one billion ounces of gold could have been transported. Although dependent upon a number of poorly known factors, this estimate considerably exceeds alternative models where limits on the gold resource would be imposed by magmatic volumes or by the amount of metamorphic fluid (cf. Fig. 3). Inefficiencies at the source (e.g., unfavorable lithologies), during transport (Cl-bearing fluids, insufficient permeability, or channeling of fluids), and during deposition (inadequate focusing or chemistry), as well as depletion of gold in low-grade source rocks, could reduce the amount of gold available as a recoverable resource, but considering that the Carlin trend alone may contain 100 Moz, this estimate appears reasonable.

Regional distribution of Carlin-type systems: In North America, the hydrothermal systems that form Carlin-type deposits may be largely restricted to the central part of the northern Basin and Range province. This region represents the coincidence of adequate energy drive with favorable source rocks. With the exception of the Caborca terrane of Sonora, which hosts a few Carlin-like deposits (Staudé, 1995; Fig. 1) and southern Idaho, other areas of high extension have either (1) thinner basement sequences which are dominated by carbonate rocks (e.g., southern Nevada, southwestern Utah), (2) dominantly (meta)igneous or pelitic lithologies (e.g., Arizona, southeastern California, western Nevada; east-central California, respectively), or (3) high-grade metasedimentary rocks (e.g., northern Mojave). None of these lithologic suites would provide a chemically favorable source. Elsewhere, suitable source lithologies (e.g., Great Valley sequence of central California) lack any major extension to drive fluid flow; instead gold mineralization may be sourced from these rocks only where igneous activity is superimposed (e.g., in the Coast Ranges as at McLaughlin; Sherlock et al., 1995).

Conversely, where suitable dilute waters are not present, gold transport may be limited by the stability of $\text{Au}(\text{HS})_2^-$. Connate fluids with their higher salinities would transport base metals but not gold (Fig. 7C) and would have to be flushed from the system before dilute fluids would predominate. Fluid inclusions from Carlin (Kuehn and Rose, 1992) indicate that such an event might have occurred in the pre-gold history of that area. Likewise, the temperate paleoclimate of the late Eocene and early Oligocene of the northern Basin and Range, which had abundant fresh water, contrasts with the arid paleoclimate and associated saline fluids during late Oligocene to Miocene extension in the southern Basin and Range (Chase et al., in press). Secular contrasts in fluids as well as differing host rocks may account for the highly

oxidized (hematite-rich) "detachment" gold-copper mineralization to the south.

Our calculations show that many lithologies can produce fluids which have the potential to form gold deposits. The complex interplay between source chemistry and deposit-level processes precludes specific identification of material sources and depositional mechanisms barring case-specific geologic and geochemical constraints. Indeed, much of the variation among deposits, particularly with regard to grade and carbonate leaching history, may indicate that the source rocks for the different districts have a substantial range in composition.

Comparison with detachment-type deposits: The contrast in source rocks, available fluids, and energy sources helps rationalize the timing and characteristics of other types of extension-related mineralization and some other metallogenic features of the Basin and Range province. Detachment-type gold systems occur in the southern Basin and Range and have a chemistry and distribution complimentary to those of Carlin-type systems (Fig. 1). They are characterized by a close structural association with high degrees of regional extension, hematite \pm copper-rich breccias, quartz, and associated potassic and hydrolytic alteration in feldspathic hosts (Wilkins et al., 1986; Roddy et al., 1988; Spencer and Welty, 1989). Geochemical evidence indicates that they formed from saline fluids of surface derivation (Kerrick et al., 1984; Wilkins et al., 1986). The high salinities (consistent with paleoclimate and Miocene evaporites), moderately oxidized feldspathic sources, and moderate temperatures indicated for these systems all contrast with the conditions assumed for the adjacent environments which generated the Carlin-type deposit, but support the idea that extensional tectonics can lead to the development of low-temperature hydrothermal systems capable of scavenging and recycling metals.

Synopsis and Conclusions

Synopsis of model and results

Geologic evidence from Carlin-type gold deposits is consistent with a mid-Tertiary age linked to crustal extension, but without a close link to coeval magmatism (Seedorff, 1991). Apparent restriction of Carlin-type systems to low metamorphic-grade portions of the Paleozoic miogeocline points to a provenance link. Geochemical data indicate that deposits formed at about 200°C under slightly acidic, fairly reduced conditions from sedimentary rock-exchanged meteoric fluids. These observations are best explained by a model of deep meteoric fluid circulation, driven by extensional thermal relaxation and increases in permeability, through the thick miogeoclinal sedimentary package of the northern Basin and Range province. Upwelling fluids of multiple types can generate the characteristic carbonate-leaching, silica-addition alteration found in carbonate host rocks. The model of extension-driven fluid flow rationalizes the provincial control, large volume, and geochemical features of Carlin-type deposits and predicts the contrasts with other deposit types in southwestern North America.

Physical and chemical evidence and reasoning support an extension-related origin. Extension-related fluid flow is amply documented in metamorphic core complexes throughout the

Basin and Range province. The mass of fluid that could be heated by this process is many times the mass needed to account for observed alteration and mineralization. In contrast, alternative causes of fluid circulation, either magmatic or metamorphic, are more severely constrained. At best, they are marginally adequate to account for the observed hydrothermal effects.

Our geochemical modeling indicates that deeply circulated meteoric fluids can leach and transport gold, sulfur, silica, and other constituents from underlying sedimentary rocks. Cooling, interaction with host rocks, and/or mixing with a second fluid at higher stratigraphic levels can lead to the precipitation of gold and quartz and leaching of carbonate minerals. Near-neutral, low-chlorinity fluids are most effective at generating high gold and low base metal contents, suggesting that arkosic rocks are the best source lithology. Under many scenarios, only arkosic fluids precipitate gold at the deposit level, suggesting an important source-rock control in the generation of barren and mineralized jasperoids. Fluids generated by metamorphic devolatilization are chemically plausible but probably unimportant in Carlin-type systems because of the lack of evidence for a coeval prograde metamorphic event and the difficulty in generating the necessary mass of fluid.

Implications and future directions

This model rationalizes the distribution of Carlin-type deposits in the central Great Basin and perhaps smaller areas in Sonora and Idaho based on the presence of plausible source rocks and regional extension as a driving force. The chemical aspects of our model share features with models proposed for Mother Lode-type gold systems (Nesbitt and Muehlenbachs, 1989). The importance of moderate sulfur, high CO₂, low-chlorinity fluids in the formation of moderate- to low-temperature gold deposits seems to provide a geochemical connection between many gold deposits (Phillips and Powell, 1993), even though the geologic processes which led to the development and circulation of these fluids can be quite different. Thus, "Carlin-like" deposits (i.e., those formed by leaching of constituents from large masses of sedimentary rocks) might be present in other sedimentary terranes where different geologic processes led to widespread thermal anomalies, as well as in other extensional environments.

The models presented here, although broadly consistent with the available evidence, point to a number of opportunities for testing and broader research:

1. Better constraints on timing of mineralization are critical to this, as well as to alternative models.
2. Flow paths and alteration at district and larger scales are needed to test links to possible source regions. For example, can flow in highly extended domains (e.g., core complexes) be tied to flow in areas (typically less extended) that host Carlin-type mineralization? Alternative material sources and flow paths should differ in metal contents and alteration styles—can they be recognized?
3. Geochemical studies at geologically well-constrained deposits are needed to determine which precipitation mechanisms are most important. It is particularly important to study

diverse examples of these systems, notably those found in unconventional hosts (e.g., contact aureoles, intrusions, red beds, basalts).

4. At the broadest scale, investigation of the hydrodynamics and chemical evolution of fluids during major extension would be useful. How do these differ in flows in other environments and what are the implications for the development of different styles of extension-related mineralization (e.g., detachment type)?

Acknowledgments

Our thinking on Carlin-type deposits has been stimulated by conversations with numerous individuals over many years, notably Eric Seedorff, Al Hofstra, and Walter Schull. We thank Paul Barton and Barbara Bekken for helpful reviews of earlier drafts of these ideas. We much appreciate comments from three *Economic Geology* reviewers and Jennifer Becker on the final versions of the manuscript. This project was supported by grants from Amselco Exploration and the National Science Foundation (EAR86-07542 and EAR90-96294).

June 3, 1996; May 28, 1997

REFERENCES

- Alvarez, A.A., and Noble, D.C., 1988, Sedimentary rock-hosted disseminated precious metal mineralization at Purisima Concepcion, Yauricocha district, central Peru: *ECONOMIC GEOLOGY*, v. 83, p. 1368–1378.
- Arehart, G.B., Kesler, S.E., O'Neil, J.R., and Foland, K.A., 1992, Evidence for the supergene origin of alunite in sediment-hosted micron gold deposits, Nevada: *ECONOMIC GEOLOGY*, v. 87, p. 263–270.
- Arehart, G.B., Foland, K.A., Naeser, C.W., and Kesler, S.E., 1993a, ⁴⁰Ar/³⁹Ar, K/Ar, and fission track geochronology of the sediment-hosted disseminated gold deposits at Post-Betze, Carlin trend, northeastern Nevada: *ECONOMIC GEOLOGY*, v. 88, p. 622–646.
- Arehart, G.B., Eldridge, C.S., Chrysosoulis, S.L., and Kesler, S.E., 1993b, Ion microprobe determination of sulfur isotope variation in iron sulfides from the Post/Betze sediment-hosted disseminated gold deposit, Nevada, USA: *Geochimica et Cosmochimica Acta*, v. 57, p. 1505–1519.
- Bagby, W.C., and Berger, B.R., 1985, Geologic characteristics of sediment-hosted, disseminated precious-metal deposits of the western United States: *Reviews in Economic Geology*, v. 2, p. 169–202.
- Bakken, B.M., 1990, Gold mineralization, wall-rock alteration, and the geochemical evolution of the hydrothermal system in the main ore body, Carlin mine, Nevada: Unpublished Ph.D. thesis, Stanford University, 236 p.
- Bakken, B.M., and Einaudi, M.T., 1986, Spatial and temporal relation between wall-rock alteration and gold mineralization, Main pit, Carlin gold mine, Nevada, U.S.A., in MacDonald, A.J., ed., *Proceedings of Gold '86*: Willowdale, Ontario, Konsult International, p. 388–403.
- Barton, M.D., 1990, Cretaceous magmatism, mineralization and metamorphism in the east-central Great Basin: *Geological Society of America Special Paper* 174, p. 283–302.
- Barton, M.D., Battles, D.A., Bebout, G.E., Capo, R.C., Christensen, J.N., Davis, S.R., Hanson, R.B., Michelsen, C.J., and Trim, H.E., 1988, Mesozoic contact metamorphism in the Western United States, in Ernst, W.G., ed., *Metamorphism and crustal evolution of the western United States*, Rubey Volume 7: Englewood Cliffs, NJ, Prentice-Hall, p. 110–178.
- Barton, M.D., Seedorff, C.E., and Ilchik, R.P., 1993, Contrasting siliceous replacement mineralization, east-central Nevada [abs.]: *Geological Society of America Abstracts with Programs*, v. 25, no. 5, p. 7.
- Barton, P.B., Bethke, P.M., and Roedder, E., 1977, Environment of ore deposition in the Creede mining district, San Juan Mountains, Colorado: Part III. Progress toward interpretation of the chemistry of ore-forming fluid in the OH vein: *ECONOMIC GEOLOGY*, v. 72, p. 1–24.
- Beatty, D.W., Landis, G.P., and Thompson, T.B., 1990, Carbonate-hosted sulfide deposits of the central Colorado mineral belt: *ECONOMIC GEOLOGY MONOGRAPH* 7, 424 p.
- Benning, L.G., and Seward, T.M., 1996, Hydrosulphide complexing of Au(I)

- in hydrothermal solutions from 150–400°C and 500–1500 bar: *Geochimica et Cosmochimica Acta*, v. 60, p. 1849–1871.
- Brown, K.L., 1986, Gold deposition from geothermal discharges in New Zealand: *ECONOMIC GEOLOGY*, v. 81, p. 979–983.
- Buck, W.R., Martinez, F., Steckler, M., and Cochran, J., 1988, Thermal consequences of lithospheric extension: Pure and simple: *Tectonics*, v. 7, p. 213–234.
- Cathles, L.M., 1981, Fluid flow and genesis of hydrothermal ore deposits: *ECONOMIC GEOLOGY 75TH ANNIVERSARY VOLUME*, p. 424–457.
- Chase, C.G., Gregory, K.M., Parrish, J.T., and DeCelles, P.G., in press, Topographic history of the western Cordillera of North America and the controls of climate: in Crowley, T. J., and Burke, K., eds., *Tectonic conditions for climate reconstruction*: Oxford University Press.
- Cline, J.S., Hofstra, A.H., and Landis, G.P., 1993, Mineral paragenesis and P T X of ore fluids at the Getchell Carlin type gold deposit, Nevada [abs.]: *Geological Society of America Abstracts with Programs*, v. 25, no. 5, p. 21.
- Cunningham, C.G., 1988, The relationship between some disseminated gold deposits and the western edge of the Precambrian craton and paleothermal anomalies in Nevada, in Schafer, R.W., Cooper, J.J., and Vikre, P.G., eds., *Bulk mineable precious metal deposits of the western United States*: Reno, Geological Society of Nevada, p. 35–48.
- Daly, W.E., Doe, T.C., and Loranger, R.J., 1991, Geology of the northern Independence Mountains, Elko County, Nevada, in Raines, G.L., Lisle, R.E., Schafer, R.W., and Wilkinson, W.H., eds., *Geology and ore deposits of the Great Basin*. Symposium proceedings: Reno, Geological Society of Nevada, v. 1, p. 583–602.
- Dickinson, W.R., 1991, Tectonic setting of faulted Tertiary strata associated with the Catalina core complex in southern Arizona: *Geological Society of America Special Paper* 264, 106 p.
- Dobra, J.L., and Thomas, P.R., 1995, The U.S. gold industry 1994: Nevada Bureau of Mines and Geology Special Publication 18, 32 p.
- Dokka, R.K., and Baksi, A.K., 1988, Thermochronology and geochronology detachment faults of the Mojave extensional belt, California: A progress report [abs.]: *Geological Society of America Abstracts with Programs*, v. 20, p. A16.
- Frantz, J.D., Popp, R.K., and Boctor, N.Z., 1981, Mineral solution equilibria—V. Solubilities of rock-forming minerals in supercritical fluids: *Geochimica et Cosmochimica Acta*, v. 45, p. 69–77.
- Fricke, H.C., Wickham, S.M., and O'Neil, J.R., 1992, Oxygen and hydrogen isotope evidence for meteoric water infiltration during mylonitization and uplift in the Ruby Mountains-East Humboldt Range core complex, Nevada: *Contributions to Mineralogy and Petrology*, v. 111, p. 203–221.
- Gans, P.B., and Miller, E.L., 1983, Style of mid-Tertiary extension in east-central Nevada: *Geological Society of America Field Tour Guidebook, Utah Geological and Mineral Survey Special Studies*, v. 59, p. 107–160.
- Gans, P.B., Mahood, G.A., and Schermer, E., 1989, Synextensional magmatism in the Basin and Range province: A case study from the eastern Great Basin: *Geological Society of America Special Paper* 233, 53 p.
- Hanson, R.B., 1995, The hydrodynamics of contact metamorphism: *Geological Society of America Bulletin*, p. 595–611.
- Hayashi, K., and Ohmoto, H., 1991, Solubility of gold in NaCl and H₂S-bearing aqueous solutions at 250–350°C: *Geochimica et Cosmochimica Acta*, v. 55, p. 2111–2126.
- Helgeson, H.C., 1979, Mass transfer among minerals and hydrothermal solutions, in Barnes, H.L., ed., *Geochemistry of hydrothermal ore deposits*, 2nd edition: New York, Wiley Interscience, p. 568–610.
- Helgeson, H.C., Kirkham, D.H., and Flowers, G.C., 1981, Theoretical prediction of the thermodynamic properties of aqueous electrolytes at high pressures and temperatures: IV. Calculation of activity coefficients, osmotic coefficients and apparent molar and standard and relative partial molar properties to 600°C and 5 kb: *American Journal of Science*, v. 281, p. 1249–1516.
- Hofstra, A.H., 1994, Geology and genesis of the Carlin-type gold deposits in the Jerritt Canyon district, Nevada: Unpublished Ph.D. Dissertation, Boulder, University of Colorado, 720 p.
- Hofstra, A.H., Northrop, H.R., Landis, G.P., Rye, R.O., and Birak, D.J., 1988, Origin of sediment-hosted gold deposits by fluid mixing—evidence from jasperoids in the Jerritt Canyon gold district [abs.]: *Bicentennial Gold '88*, Melbourne, Australia, May, 1988, Extended Oral Abstracts, p. 284–289.
- Hofstra, A.H., Leventhal, J.S., Northrop, H.R., Landis, G.P., Rye, R.O., Birak, D.J., and Dahl, A.R., 1991, Genesis of sediment-hosted disseminated-gold deposits by fluid mixing and sulfidation; chemical-reaction-path modeling of ore-depositional processes documented in the Jerritt Canyon district, Nevada: *Geology*, v. 19, p. 36–40.
- Holland, P.T., Beatty, D.W., and Snow, G.G., 1988, Comparative elemental and oxygen isotope geochemistry of jasperoid in the northern Great Basin; evidence for distinctive fluid evolution in gold-producing hydrothermal systems: *ECONOMIC GEOLOGY*, v. 83, p. 1401–1423.
- Ilchik, R.P., 1990a, Geology and geochemistry of the Vantage gold deposits, Alligator Ridge-Bald Mountain mining district, Nevada: *ECONOMIC GEOLOGY*, v. 85, p. 50–75.
- 1990b, Geology and genesis of the Vantage gold deposits, Alligator Ridge-Bald Mountain mining district, Nevada: Unpublished Ph.D. thesis, University of California, Los Angeles, 155 p.
- 1995, ⁴⁰Ar/³⁹Ar, K/Ar, and fission track geochronology of the sediment-hosted disseminated gold deposits at Post-Betze, Carlin trend, northeastern Nevada—a discussion: *ECONOMIC GEOLOGY*, v. 90, p. 208–210.
- Ilchik, R.P., and Barton, M.D., 1996, Physical and chemical constraints for an amagmatic origin of Carlin-type gold deposits, a source-sink approach: *Geological Society of Nevada Symposium*, Reno/Sparks, Nevada, April 1995, p. 687–708.
- Johnson, J.W., Olkers, E.H., and Helgeson, H.C., 1992, SUPCRT92: A software package for calculating the standard molal thermodynamic properties of minerals, gases, aqueous species and reactions from 1 to 5000 bars and 0° to 1000°C: Berkeley, University of California, Laboratory of Theoretical Geochemistry.
- Joralemon, P., 1951, The occurrence of gold at the Getchell mine, Nevada: *ECONOMIC GEOLOGY*, v. 46, p. 267–310.
- Keays, R.R., Ramsay, W.R.H., and Groves, D.J., 1989, The geology of gold deposits: The perspective in 1988: *ECONOMIC GEOLOGY MONOGRAPH* 6, 667 p.
- Kerrick, R., and Rehrig, W., 1987, Fluid motion associated with Tertiary mylonitization and detachment faulting: 18O/16O evidence from the Picacho metamorphic core complex, Arizona: *Geology*, v. 15, p. 58–62.
- Kerrick, R., Rehrig, W.A., Willmore, L.M., 1984, Deformation and hydrothermal regimens in the Picacho metamorphic core complex detachment-Arizona: Oxygen isotope evidence [abs.]: *EOS*, v. 65, p. 1124.
- Kuehn, C.A., and Rose, A.W., 1992, Geology and geochemistry of wall-rock alteration at the Carlin gold deposit, Nevada: *ECONOMIC GEOLOGY*, v. 87, p. 1697–1721.
- 1995, Carlin gold deposit, Nevada: Origin in a deep zone of mixing between normally pressured and overpressured fluids: *ECONOMIC GEOLOGY*, v. 90, p. 17–36.
- Lamb, J.B., and Cline, J.S., 1993, Mineral paragenesis and fluid inclusion study of the Meikle mine, Carlin, Nevada [abs.]: *Geological Society of America Abstracts with Programs*, v. 25, no. 5, p. 65–66.
- Lee, D.E., Friedman, L., and Gleason, J.D., 1984, Modification of dD values in eastern Nevada granitoid rocks spatially related to thrusting: *Contributions to Mineralogy and Petrology*, v. 88, p. 288–298.
- Maher, D., 1996, Stratigraphy, structure and alteration of igneous and carbonate wall rocks at Veteran Extension in the Robinson (Ely) porphyry copper district, Nevada: *Geological Society of Nevada Symposium*, Reno/Sparks, Nevada, April 1995, p. 1595–1621.
- Maher, B.J., Browne, Q.J., and McKee, E.H., 1993, Constraints on the age of gold mineralization and metallogenesis in the Battle Mountain-Eureka mineral belt, Nevada: *ECONOMIC GEOLOGY*, v. 88, p. 469–478.
- Matthäi, S.K., Henley, R.W., Bacigalupo-Rose, S., Binns, R.A., Andrew, A.S., Carr, G.R., French, D.H., McAndrew, J., and Kananagh, M.E., 1995, Intrusion-related, high-temperature gold quartz veining in the Cosmopolitan Howley gold deposit, Northern Territory, Australia: *ECONOMIC GEOLOGY*, v. 90, p. 1012–1045.
- Miller, D.M., Hillhouse, W.C., Zartman, R.E., and Lanphere, M.A., 1987, Geochronology of intrusive and metamorphic rocks in the Pilot Range, Utah and Nevada, and comparison with regional patterns: *Geological Society of America Bulletin*, v. 99, p. 866–879.
- Miller, E.L., Gans, P.B., Wright, J.E., and Sutter, J.F., 1988, Metamorphic history of the east-central Basin and Range province: Tectonic setting and relationships to magmatism, in Ernst, W.G., ed., *Metamorphism and crustal evolution of the western United States*, Rubey Volume 7: Englewood Cliffs, NJ, Prentice-Hall, p. 649–682.
- Miller, E.L., Miller, M.M., Stevens, C.H., Wright, J.E., and Madrid, R., 1992, Plate Paleozoic paleogeographic and tectonic evolution of the western US cordillera: Boulder, Colorado, Geological Society of America, *The Geology of North America*, v. G-3, p. 57–106.

- Misch, P., and Hazzard, J.C., 1962, Stratigraphy and metamorphism of Late Precambrian rocks in central northeastern Nevada and adjacent Utah: *American Association of Petroleum Geologists Bulletin*, v. 46, p. 289–343.
- Nordstrom, D.K., and Munoz, J.L., 1994, *Geochemical thermodynamics*, 2nd edition: Cambridge, Massachusetts, Blackwell Scientific Publications, 493 p.
- Norton, D., 1982, Fluid and heat transport phenomena typical of copper-bearing pluton environments; southeastern Arizona, in Titley, S.R., ed., *Advances in geology of porphyry copper deposits, southwestern North America*: Tucson, University of Arizona Press, p. 59–72.
- Nesbitt, B.E., and Muehlenbachs, K., 1989, Geology, geochemistry, and genesis of mesothermal gold deposits of the Canadian Cordillera: Evidence for ore formation from evolved meteoric water: *ECONOMIC GEOLOGY MONOGRAPH* 6, p. 553–563.
- Paul, E.K., Muirhead, E.M.M., and Kunkel, K.W., 1993, Geology and gold mineralization of the Genesis deposit, Eureka County, Nevada: *Society of Economic Geologists Guidebook*, v. 18, p. 36–49.
- Pearson, M., and Garven, G., 1994, A sensitivity study of the driving forces on fluid flow during continental-rift basin evolution: *Geological Society of America Bulletin*, v. 106, p. 461–475.
- Percival, T.J., Bagby, W.C., and Radtke, A.S., 1988, Physical and chemical features of precious metal deposits hosted by sedimentary rocks in the western United States, in Schafer, R.W., Cooper, J.J., and Vikre, P.G., eds., *Bulk mineable precious metal deposits of the western United States*: Reno, Geological Society of Nevada, p. 11–34.
- Phillips, G.N., and Powell, R., 1993, Link between gold provinces: *ECONOMIC GEOLOGY*, v. 88, p. 1084–1098.
- Phinisey, J.D., 1995, Petrography, alteration and mineralization of igneous dikes of the Jerritt Canyon district, Elko County, Nevada: Unpublished M.Sc. thesis, Reno, University of Nevada, 173 p.
- Radtke, A.S., Rye, R.O., and Dickson, F.W., 1980, Geology and stable isotope studies of the Carlin gold deposit, Nevada: *ECONOMIC GEOLOGY*, v. 75, p. 641–672.
- Raines, G.L., Lisle, R.E., Schafer, R.W., and Wilkinson, W.H., eds., 1991, *Geology and ore deposits of the Great Basin*. Symposium proceedings: Reno, Geological Society of Nevada, 1257 p.
- Reed, M.H., and Spycher, N.F., 1990, *Soltherm: Data base of equilibrium constants for aqueous-mineral-gas equilibria*: University of Oregon, Department of Geological Sciences.
- Rimstidt, J.D., and Barnes, H.L., 1980, The kinetics of silica-water reactions: *Geochimica et Cosmochimica Acta*, v. 44, p. 1683–1699.
- Roberts, R.J., 1966, Metallogenic provinces and mineral belts in Nevada: *Nevada Bureau of Mines Report* 13, p. 47–72.
- Roberts, R.J., Radtke, A.S., and Coats, R.R., 1971, Gold-bearing deposits in north-central Nevada and southwestern Idaho: *ECONOMIC GEOLOGY*, v. 66, p. 14–33.
- Roddy, M.S., Reynolds, S.J., Smith, B.M., and Ruiz, J., 1988, K-metamorphism and detachment-related mineralization, Harcuvar Mountains, Arizona: *Geological Society of America Bulletin*, v. 100, p. 1627–1639.
- Rye, R.O., 1985, A model for the formation of carbonate-hosted disseminated gold deposits based on geologic, fluid-inclusion, geochemical, and stable-isotope studies of the Carlin and Cortez deposits, Nevada: *U.S. Geological Survey Bulletin* 1646, p. 95–105.
- Rye, R.O., Doe, B.R., and Wells, J.D., 1974, Stable isotope and lead isotope study of the Cortez, Nevada, gold deposit and surrounding area: *U.S. Geological Survey Journal of Research*, v. 2, p. 13–23.
- Saleeby, J.B., Busby-Spera, C.J., Oldow, J.S., Dunne, G.C., Wright, J.E., Cowan, D.S., Walker, N.W., and Allmendinger, R.W., 1992, Early Mesozoic tectonic evolution of the western United States cordillera: Boulder, Colorado, Geological Society of America, *The Geology of North America*, v. G-3, p. 107–168.
- Seedorff, E., 1991, Magmatism, extension, and ore deposits of Eocene to Holocene age in the Great Basin: mutual effects and preliminary proposed genetic relationships, in Raines, G.L., Lisle, R.E., Schafer, R.W., and Wilkinson, W.H., eds., *Geology and ore deposits of the Great Basin*. Symposium proceedings: Reno, Geological Society of Nevada, v. 1, p. 133–178.
- Seward, T.M., 1973, Thiocomplexes of gold and the transport of gold in hydrothermal ore solutions: *Geochimica et Cosmochimica Acta*, v. 37, p. 379–399.
- Shenberger, D.M., and Barnes, H.L., 1989, Solubility of gold in aqueous sulfide solutions from 150 to 350°C: *Geochimica et Cosmochimica Acta*, v. 53, p. 269–278.
- Sherlock, R.L., Tosdal, R.M., Lehrman, N.J., Graney, J.R., Losh, S., Jowett, E.C., and Kesler, S.E., 1995, Origin of the McLaughlin mine sheeted vein complex: Metal zoning, fluid inclusion, and isotopic evidence: *ECONOMIC GEOLOGY*, v. 90, p. 2156–2181.
- Silberman, M.L., Berger, B.R., and Koski, R.A., 1974, K-Ar relations of granodiorite emplacement and tungsten and gold mineralization near the Getchell mine, Humboldt County, Nevada: *ECONOMIC GEOLOGY*, v. 69, p. 646–656.
- Sillitoe, R.H., 1988, Gold and silver deposits in porphyry systems, in Schafer, R.W., Cooper, J.J., and Vikre, P.G., eds., *Bulk mineable precious metal deposits of the western United States*: Reno, Geological Society of Nevada, p. 233–257.
- Sillitoe, R.H., and Bonham, H.F., Jr., 1990, Sediment-hosted gold deposits: distal products of magmatic-hydrothermal systems: *Geology*, v. 18, p. 157–161.
- Smith, M.R., Wilson, W.R., Benham, J.A., Pescio, C.A., and Valenti, P., 1988, The Star Pointer gold deposit, Robinson mining district, White Pine County, Nevada, in Schafer, R.W., Cooper, J.J., and Vikre, P.G., eds., *Bulk mineable precious metal deposits of the western United States*: Reno, Geological Society of Nevada, p. 221–231.
- Snook, A.W., and Miller, D.M., 1988, Metamorphic and tectonic history of the northeastern Great Basin, in Ernst, W.G., ed., *Rubey Volume 7: Englewood Cliffs, NJ, Prentice-Hall*, p. 606–648.
- Spencer, J.E., and Welty, J.W., 1989, Mid-Tertiary ore deposits in Arizona: *Arizona Geological Society Digest* 17, p. 585–607.
- Spycher, N.F., and Reed, M.K., 1989, Evolution of a Broadlands-type epithermal ore fluid along alternative P-T paths: Implications for the transport and deposition of base, precious and volatile metals: *ECONOMIC GEOLOGY*, v. 84, p. 328–359.
- Staude, J.M.G., 1995, Epithermal mineralization in the Sierra Madre Occidental, and the metallogeny of northwestern Mexico: Unpublished Ph.D. thesis, University of Arizona, 248 p.
- Stewart, J.H., 1980, *Geology of Nevada*: Nevada Bureau of Mines and Geology Special Publication 4, 136 p.
- Stewart, J.H., and Carlson, J.E., 1978, *Geologic map of Nevada*: Nevada Bureau of Mines and Geology, scale 1:500,000.
- Sverjensky, D.A., Hemley, J.J., and d'Angelo, W.M., 1991, Thermodynamic assessment of hydrothermal alkali feldspar-mica-aluminosilicate equilibria: *Geochimica et Cosmochimica Acta*, v. 55, p. 989–1004.
- Thorman, C.H., Ketner, K.B., Brooks, W.E., Snee, L.W., and Zimmerman, R.A., 1991, Late Mesozoic-Cenozoic tectonics in northeastern Nevada, in Raines, G.L., Lisle, R.E., Schafer, R.W., and Wilkinson, W.H., eds., *Geology and ore deposits of the Great Basin*. Symposium proceedings: Geological Society of Nevada, v. 1, p. 25–45.
- Tooker, E.W., 1985, Geologic characteristics of sediment- and volcanic-hosted disseminated gold deposits—search for an occurrence model: *U.S. Geological Survey Bulletin* 1646, 150 p.
- Turcotte, D.L., and Schubert, G., 1982, *Geodynamics: Application of continuum physics to geological problems*: New York, Wiley, 450 p.
- Van Zeggeren, F., and Storey, S.H., 1970, *The computation of chemical equilibria*: Cambridge, Cambridge University Press, 176 p.
- Wrucke, C.T., and Armbrustermacher, T.J., 1975, Geochemical and geologic relations of gold and other elements at the Gold Acres open-pit mine, Lander County, Nevada: *U.S. Geological Survey Professional Paper* 860, 27 p.
- Wells, D.E., and Mullens, T.E., 1973, Gold-bearing Arsenian pyrite determined by microprobe analysis, Cortez and Carlin gold mines, Nevada: *ECONOMIC GEOLOGY*, v. 68, p. 187–201.
- Willden, R., 1964, Geology and mineral deposits of Humboldt County, Nevada: *Nevada Bureau of Mines and Geology Bulletin* 59, 154 p.
- Wilkins, J., Jr., Beane, R.E., and Hiedrick, T.L., 1986, Mineralization related to detachment faults: A model: *Arizona Geological Society Digest*, v. 16, p. 108–117.
- Wilson, P.N., and Parry, W.T., 1995, Characterization and dating of argillic alteration in the Mercur gold district, Utah: *ECONOMIC GEOLOGY*, v. 90, p. 1197–1216.
- Zoback, M.L., and Thompson, G.A., 1978, Basin and Range rifting in northern Nevada: Clues from a mid-Miocene rift and its subsequent offsets: *Geology*, v. 6, p. 111–116.
- Zotov, A.V., Baranova, N.N., Dar'yina, T.G., and Bannykh, L.M., 1991, The solubility of gold in aqueous chloride fluids at 350–500°C and 500–1500 Atm: Thermodynamic parameters of AuCl₂(sol) up to 750°C and 5000 Atm: *Geochemistry International*, v. 28, no. 2, p. 63–71.